JHR 98: 435–465 (2025)
doi: 10.3897/jhr.98.141572
https://jhr.pensoft.net

RESEARCH ARTICLE

JOURNAL OF Hymenoptera RESEARCH
A peer-reviewed open-access journal
The International Society of Hymenopterists

Comparative morphological analysis of mature larvae of eight *Vespa* Linnaeus, 1758 species (Hymenoptera, Vespidae) in South Korea

Jaehee Kim[1], Oh-Seok Kwon[2], Seiki Yamane[3], Moon Bo Choi[4]

1 *Department of Applied Biology, College of Agriculture and Life Sciences, Kyungpook National University, Daegu, Republic of Korea* **2** *Department of Plant Medicine, College of Agriculture and Life Sciences, Kyungpook National University, Daegu, Republic of Korea* **3** *Haruyama-chô 1054-1, Kagoshima-shi 899-2704, Japan* **4** *Institute of Agricultural Science and Technology, Kyungpook National University, Daegu, Republic of Korea*

Corresponding authors: Moon Bo Choi (kosinchoi@hanmail.net); Seiki Yamane (mayiopa0@gmail.com)

Academic editor: Michael Ohl | Received 11 November 2024 | Accepted 27 March 2025 | Published 8 April 2025

https://zoobank.org/57580D57-10C7-4FE2-A997-624E3CE20BE5

Citation: Kim J, Kwon O-S, Yamane S, Choi MB (2025) Comparative morphological analysis of mature larvae of eight *Vespa* Linnaeus, 1758 species (Hymenoptera, Vespidae) in South Korea. Journal of Hymenoptera Research 98: 435–465. https://doi.org/10.3897/jhr.98.141572

Abstract

The social wasp genus *Vespa*, encompassing insects commonly referred to as hornets, consists of 22 species that are predominantly distributed across the Palearctic and Indomalayan regions. These harmful pests, often spread through trade, pose risks to public health. Hornet larvae undergo development within the protected environment of nests. Hence, they may exhibit more conserved characteristics than adults, which face direct selection pressure. To date, larval morphology has been studied in only approximately half of the 22 known hornet species, and in-depth comparative research on species within the genus *Vespa* is scarce. In South Korea, comprehensive descriptions and identification keys for the eight reported species and two subspecies are lacking. To address this gap, this study aimed to provide morphological descriptions and identification characteristics of mature larvae from eight *Vespa* species in South Korea. Between 2021 and 2024, larvae were collected from nests across South Korea. The larvae were observed under scanning electron microscopy, optical microscopy, and stereo microscopy to evaluate various morphological characteristics. Results indicated that distinguishing hornet larvae morphologically from larvae of other taxonomic groups is challenging. Specifically, no significant morphological differences were noted between *V. velutina nigrithorax* and *V. simillima simillima*. The lack of distinctive morphological features in larvae complicates taxonomic identification, making it more challenging compared to the identification of adult specimens.

Keywords

Korean hornet, Larval morphology, taxonomic analysis, *Vespa* species

Copyright *Jaehee Kim et al.* This is an open access article distributed under the terms of the Creative Commons Attribution License (CC BY 4.0), which permits unrestricted use, distribution, and reproduction in any medium, provided the original author and source are credited.

Introduction

The social wasp genus *Vespa* Linnaeus, 1758 (Hymenoptera: Vespidae: Vespinae) consists of insects commonly known as hornets. This genus includes a total of 22 species that are predominantly distributed across the Palearctic and Indomalayan regions (Smith-Paldo et al. 2020). These insects are recognized as highly dangerous and problematic pests due to their defensive attacks on humans who approach their colonies. Their stings are poisonous and can cause pain and sometimes provoke severe, even fatal, allergic reactions (Matsuura and Yamane 1990; Schmidt 2018; Choi 2021). In recent years, *V. velutina nigrithorax* du Buysson, 1905 has invaded countries in East Asia and Europe (Kim et al. 2006; Lioy et al. 2022), and *V. mandarinia* Cameron, 1852 has spread to the United States (Wilson et al. 2020), making these species increasingly significant urban pests. Their ability to spread through global trade and travel (Lima et al. 2022; Otis et al. 2023), coupled with their negative impact on apiculture (Requier et al. 2023) and threats to public health (Tsai et al. 2005; Jeyanthi 2010), present serious global concerns. In South Korea, the rising number of hornet nests reported to emergency services (Choi et al. 2012, 2019) and the growing public fear of hornets (Choi et al. 2019; Landaverde and Rumble 2020; Skvarla et al. 2022) reflect the increasing aversion to these insects in modern society. Therefore, detailed ecological and taxonomic studies on hornets are crucial for the effective management of both also invasive and native hornet species.

Traditionally, taxonomic studies on hornets have primarily relied on adult morphological characteristics (Archer 1993); however, recent studies have incorporated molecular analyses to enhance accuracy (Carpenter et al. 2013; Perrard et al. 2016). Phylogenetic interpretations based on larval morphology have been explored not only for adults but also in certain Insecta taxa (Marvaldi 1997; Fleck et al. 2008), suggesting that the morphology of non-adult developmental stages can also be utilized for phylogenetic analysis. In the case of the genus *Vespa*, non-adult developmental stages, including egg, larva, pupa, and nest, have been excluded from integrative interpretations due to a lack of taxonomic knowledge. Therefore, phylogenetic trees constructed based on larval traits could provide valuable insights when compared with the existing adult-based tree (Carpenter et al. 2013).

During their developmental period, hornet larvae depend on nutritional inputs provided either by the queen during the solitary phase or by foraging workers in later stages (Matsuura and Yamane 1990; Schultner et al. 2017). Furthermore, eusocial species have evolved mechanisms to invest significant resources in the care of eggs and developing larvae or nymphs (Royle et al. 2012), including the regulation of nest temperature and humidity, structural fortification, and defense against intruders. This high degree of care can result in a more conserved larval phenotype compared to the adult form, potentially making larval morphological characteristics a valuable source of information on interspecies relationships. To date, morphological studies have been conducted on the larvae of 11 out of the 22 recognized hornet species (Reid 1942; Yamane 1976; Kojima 1998; Kojima et al. 2001; Tan et al. 2013). However, detailed species-level descriptions and data on interspecific and intersubspecific variation remain scarce. In South Korea,

eight hornet species and two subspecies have been documented, including the invasive *V. velutina nigrithorax* du Buysson, 1905 (Kim et al. 2006; Choi et al. 2013). For *V. simillima xanthoptera* Cameron, 1903, *V. simillima* and *V. crabro flavofasciata* Cameron, 1903, all recorded in South Korea (Choi et al. 2013), only pictorial identification keys are currently available (Yamane 1976). Furthermore, the literature contains only a brief description of *V. dybowskii* André (Kojima 1998). Although sporadic studies have been conducted on these species, comprehensive and systematic studies are lacking.

To address this gap, this study aimed to develop identification keys and provide detailed morphological descriptions of the mature larval stage, specifically the fifth instar, for eight hornet species, including five species indigenous to South Korea that have not been extensively studied.

Methods

Sample collection

Most morphological analyses of *Vespa* larvae have focused on fifth the instar, as their head capsules are the most sclerotized at this stage, with traits are being more distinct and observable (Spradbery 1973; Yamane 1976). Therefore, this study aimed to examine mature larvae to ensure consistency with previous studies and facilitate detailed morphological observations. Larvae were collected from nests of eight *Vespa* species in South Korea, between 2021 and 2024. For each species, more than 80 individual larvae were observed and sampled, except for *V. binghami* du Buysson, 1905, which, due to its rarity, was sampled from a single nest containing 10 individuals. Mature larvae were identified based on several key features, including body size, particularly head width, a strongly sclerotized and yellow-pigmented head, and a heavily sclerotized apical portion of the mandible. Larvae collected in 2021 and 2022 were stored in a freezer at –20 °C until processing, and those collected in 2023 and 2024 were immediately processed.

Sample treatment

All samples were dissected at the junction between the head and the first body segment, and gut contents were removed using distilled water. The head and body samples were then treated according to the protocols detailed below:

Head

The heads were cleaned with a 10% potassium hydroxide (KOH) solution. For scanning electron microscopy, three specimens per species were fixed in a 10% formaldehyde solution with a pH 6.86 phosphate buffer for 6 h and then dehydrated in a graded ethanol series, 30%, 50%, 70%, and 90%, followed by isoamyl acetate. Specimens were subsequently treated with hexamethyldisilazane (HMDS) before they were completely

dried and subjected to gold coating. Other specimens were rinsed with a 90% ethanol solution and distilled water to remove any residual KOH and then heavily stained with a 1% acid fuchsin solution. All treated samples were preserved in a 90% ethanol solution.

Body integument

The dissected bodies were cleaned with a 10% KOH solution and treated following the same protocols as those applied to the head samples.

Sample observation

Head

After fixation and complete drying, three specimens per species were imaged using a HITACHI SU8220 scanning electron microscope (Tokyo, Japan). Additional specimens were examined under a ZIMS 4K-3D stereomicroscope (Seoul, South Korea). Frontal views of the heads were captured during treatment with pure glycerol. For each species, 10 individuals were dissected to isolate the mandibles, labrums, and various cranial parts, which were mounted on slides for examination with an OLYMPUS CH20BIMF200 optical microscope (Tokyo, Japan). Specimens stored in the freezer may exhibit significant morphological changes due to dehydration. Therefore, we excluded any distinct morphological differences, such as variation in cranial reticulation, between freshly treated specimens and those stored in the freezer from our observations. To analyze the arrangement of mandibular teeth, the terminal margin was outlined, and each bifurcation point, and tooth apex were marked as a landmark. These landmarks were connected by lines to calculate angles and spatial arrangements between the points (Fig. 1).

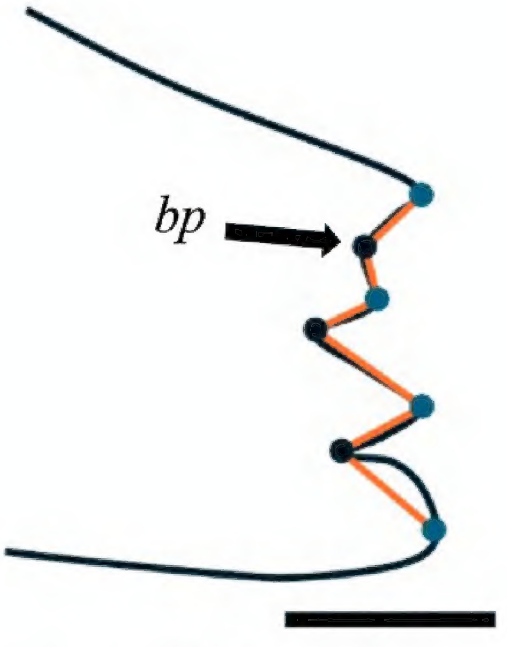

Figure 1. Apical portion of the right mandible. Black dots indicate bifurcation points (bps) between two adjacent teeth, and navy blue dots depict the apices of the teeth. Orange lines connect the black and navy blue dots. Scale bar: 0.1 mm.

Body integument

After cleaning and staining, sections of the body epidermis were taken along the dorsomedial line, mounted on slides, and examined using the aforementioned optical microscope.

Measurements and indices

Body length: roughly measured from the anterior end of the thorax to the tip of the abdomen.
Cranial width (**CW**): maximum width of the head in full frontal view.
Mandibular teeth separation: angle formed by two adjacent teeth (Fig. 1).
Mouth part width (**MW**): distance between the outermost points of the cavity where mouth parts are inserted, with the head in ventral view.
CW/MW: cranial width/mouthpart width ratio.
CLI: clypeal index; The height of the main disc is measured from its dorsal margin to a straight line drawn between the interior mandibular articulations. The height of the ventral disc is measured from this line to the ventral margin (Fig. 2).

Terminology

The terminology used in this study primarily follows Reid (1942), Yamane (1976), and Tan et al. (2013). This study mainly focused on examining and comparing the structural characteristics of the head in mature larvae.

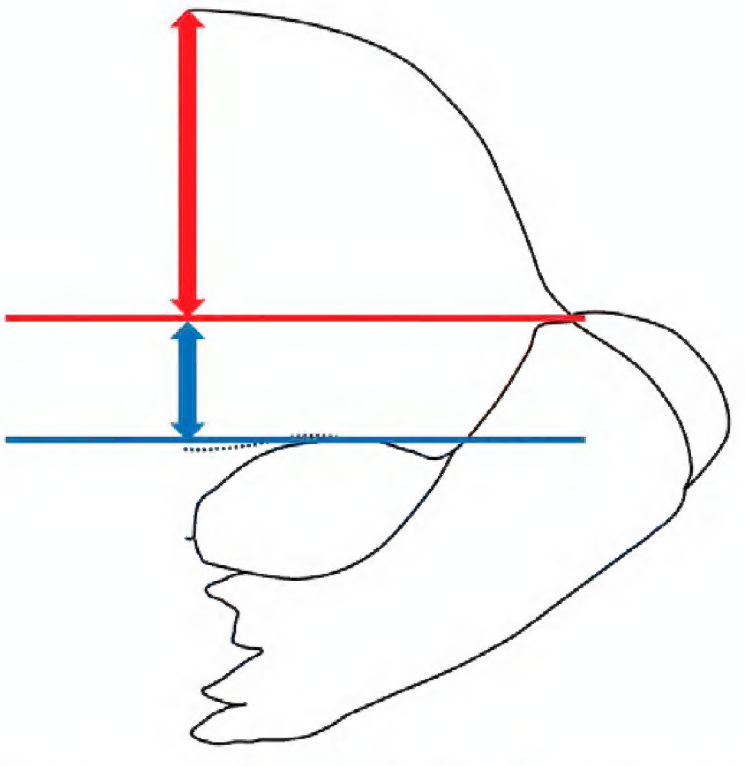

Figure 2. Left half of the clypeus and left mandible. The orange double-headed arrow indicates the height of the main disc of the clypeus (M), and the blue double-headed arrow indicates the height of the ventral section (V). The clypeal index (CLI) is defined as M/V.

List of abbreviations

(Fig. 3)

ant	antenna; circular, encircled by a slightly elevated ring (rim)
bp	bifurcation point of two adjacent mandibular teeth; the base of the cuneiform incision formed between two adjacent teeth
clp	clypeus; well-defined by an epistomal suture above and a labroclypeal suture below, comprising a dorsal (upper) main disc and a smaller ventral (lower) section. These sections are separated by a straight or curved line drawn between the interior articulations of the mandibles. The ventral section is strongly transverse and less sclerotized than the main disc.
cp	conical papillae on the palate (see *lm*)
dfm	depression on the cranium at the origin of the frontalis muscle
dt	dotted patch around the dorsalmost area of the frons; prominent in *V. simillima simillima* and *V. velutina nigrithorax*
fr	frons; triangular area laterally defined by frontal sutures and ventrally by the epistomal suture (dorsal margin of the clypeus)
ga	galea; sensory palp located on the maxillary palp (see *mplp*); however, its definition remains controversial
lcs	labroclypeal suture (see *clp*); membranous area presents between this suture and the labrum
lm	labrum; two-fold structure, with the outer surface defined as the labrum and the inner surface, known as the palate, containing numerous important characteristics
lplp	labial palp; located ventrally on the prelabium (see *prlb*)
mcs	mid-cranial suture; also known as the cleavage line
md	mandible
mp	minute pits on the labrum
mpt	median patch; darkened area on the palate, located at the median extremity of the palate
mplp	maxillary palp; located distally on the maxillary apex (see *ga*)
psm	paired suprafrontal marks; the milky branch that diverges from the mcs; located dorsally on the frontalis suture
prlb	prelabium; the anterior section of the labium, also known as the prementum
ps	punctures bearing minute setae on the labrum
sp	sclerotized patch on the palate (see **lm**)
spi	spicule; microscopic process on the palate (see **lm**)
tmb	temporal band; also known as temporal fossa, ocular fossa, or parietal band, indicating the position of the eye

Results

Vespa mandarinia Cameron, 1852

Description. ***Head*** (Fig. 3): CW/MW = 1.29–1.42 (n = 45, mean 1.39). Cranium moderately rugo-reticulated and transversely wrinkled. Antenna (***ant***) located at mid-height on the cranium, distinctly posterior to the dorsal margin of the clypeus (Fig. 3D, E), measuring 0.08 mm in width; antennal rim thin yet distinct, with weak ventrolateral margins (indicated by an arrow in Fig. 3H), and well-defined in other regions. Temporal band (***tmb***) clearly visible (Fig. 3D, E, G), with a narrow zone along its inner margin heavily pigmented with ferruginous coloration, except in the dorsal and ventral thirds. Ventral and dorsal edges distinctly margined, with remaining portions vaguely defined; ventral edge positioned slightly above the level of the dorsal margin of the antenna. Region around the frontal suture (***fs***) dorsally bearing setae (n = 7–12); frons (***fr***), except for the area near the *fs*, bearing several setae; frontal sutures originating from the mid-cranial sulcus (***mcs***) (Fig. 3E); paired suprafrontal marks (***psm***) well-defined (Fig. 3E). Faint dotted patches on the frons (Fig. 3E). Clypeus as depicted in Fig. 3D, E, G; main disc transverse, with a width exceeding the minimum distance between the antennae; dorsal margin shallowly and roundly convex and dorsolateral corners semi-angulate; lateral margin, which houses the tentorial pit, straight and without a pigmented spot; main disc relatively low, with a CLI of 1.5–2; main disc with approximately 80 setae. Labrum as shown in Fig. 3B, C, F (left), with numerous sensory bristles on its lower half. Palate (Fig. 3C, F: right) with or without a median patch (***mpt***) of variable size; sclerotized patch (***sp***, Fig. 3F) extending toward the dorsolateral corner of the palate, measuring approximately half the palate width; median area with dense conical papillae (***cp***), with the papillae sparser in the lateral area more sparsely distributed. Largest conical papilla approximately 0.03 mm in width and positioned ventrally on the palate. Spicules (***spi***) distributed on the medio-ventral portion and along the lateral margins of the palate. Mandible (***md***) with three teeth (Fig. 3A, D, I), which are heavily sclerotized with blunt apices; outer surface of the mandible entirely covered with numerous pits. Mandibular teeth I and II distinctly more projected than tooth III, which is apically bifid; Tooth I as long as tooth II, whereas tooth IIIb slightly more prominent than IIIa. Tooth I separated from II at an angle of 40°–70°, II from IIIa at 50°–70°, and IIIa from IIIb at 70°–105°. Tooth I slightly broader than II and ventrally thick; tooth II with a smooth ventral margin and a minutely gibbous dorsal margin; bifurcation point of teeth II and IIIa slightly deeper than other bifurcation points (Fig. 3H). Maxilla with approximately 25 setae, with those near the palpus being 1.5 times longer than those on other parts. Prelabium with approximately 30 setae.

Body (thorax and abdomen): Body 26–35 mm in length (n = 45, mean 31.2 mm) and 13–19 mm in width (mean 15.7 mm); integument with sparse setae and widely spaced, short spicules. Spiracles deep, generally uniform in size except for spiracles 1, 2, and 10, which are slightly smaller; largest spiracle 0.65 mm in diameter; rim of spiracle

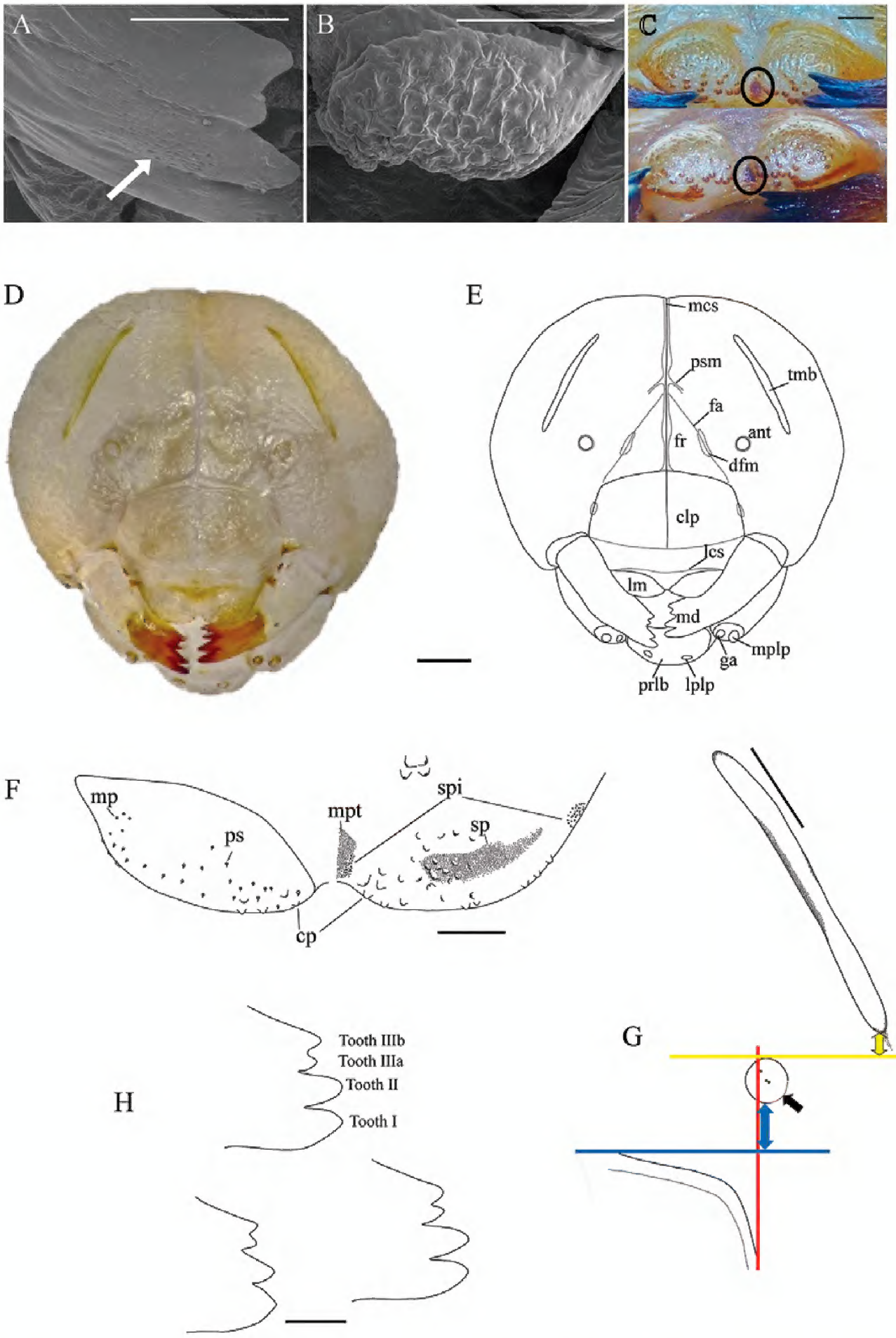

Figure 3. *Vespa mandarinia* **A** apical portion of the right mandible, with the arrow indicating pits **B** left half of the labrum in ventrofrontal view **C** two examples of the labrum (ventral view), with the median patch circled **D, E** head in frontal view **F** labrum (left) and palate (right) in frontal view **G** relative positions of the temporal band, antenna (arrow), and clypeus, with a thick double-headed arrow indicating the distance between the dorsal margin of the clypeus and the ventral margin of the antenna **H** apical portion of the mandible, showing the configuration of the teeth. (For abbreviations, see *Terminology*.) Scale bars: 0.2 mm (**A, B**); 0.1 mm (**C, F, H**); 0.3 mm (**D, E, G**).

0.06 mm in thickness, consisting of distinct, elongated processes; inner part with short and thick atrial processes.

Remarks. In this species, the CW/MW ratio is consistently below 1.45. Yamane (1976) also used this smaller CW/MW ratio to distinguish *V. mandarinia* from other *Vespa* species. The median patch on the palate is absent in the Japanese and Taiwanese populations of *V. mandarinia* (Yamane 1976); however, some Korean specimens examined in this study exhibited this feature. Although this characteristic varied among our Korean samples, it remains unclear whether it is stable in the Japanese and Taiwanese populations.

Specimens examined. South Korea • 15 mature larvae; Gwangju; 35°11'48"N, 126°53'24"E; 20 Oct. 2021; Choi and Kim • 5 mature larvae; Ulsan; 35°28'29"N, 129°11'30"E; 14 Sept. 2022; Ma • 30 mature larvae; Gyeongsangbuk-do, Uiseong-gun; 36°22'39"N, 128°38'08"E; 01 Sept. 2023; Choi and Kim • 5 mature larvae; Gyeonsangbuk-do, Uiseong-gun; 36°23'44"N, 128°26'44"E; 12 Sept. 2023; Ma • 10 mature larvae; Gyeongsangbuk-do, Gyeongju-si; 35°49'11"N, 129°18'16"E; 08 Aug. 2024; Ma • 10 mature larvae; Gangwon-do, Taebaek-si; 37°10'15"N, 128°58'16"E; 11 Sept. 2024; Choi • 15 mature larvae; Daejeon; 36°16'30"N, 127°22'33"E; 20 Sept. 2024; Choi and Kim • 20 mature larvae; Gyeongsangnam-do, Jinju-si; 35°11'10"N, 128°09'36"E; 4 Oct. 2024; Ma • 5 mature larvae; Gyeongsangbuk-do, Andong-si; 36°36'36"N, 128°48'55"E; 18 Oct. 2024; Choi.

Vespa ducalis Smith, 1852

Description. ***Head*** (Fig. 4): CW/MW = 1.6–1.74 (n = 47, mean 1.67). Cranium moderately rugo-reticulated and transversely wrinkled in the ventral area from the lateral margin of the clypeus to the outer margin of the gena. Antenna located at mid-height on the cranium, distinctly behind the dorsal margin of the clypeus (Fig. 4D, E), with a diameter of 0.09 mm and moderate sclerotization (Fig. 4D). Temporal band (Fig. 4D, E, H) generally narrow, with a heavily margined dorsal edge, moderately margined ventral edge, and poorly defined lateral margins; inner part heavily ferruginous-pigmented except in the dorsal and ventral areas (Fig. 4H). Ventral edge positioned slightly above the level of the dorsal margin of the antenna (Fig. 4E). Paired suprafrontal marks well-defined (Fig. 4E). Area around the antenna milky, with faint dotted patches on the frons. Region around the frontal suture dorsally bearing setae (n = 8–12), which are densely distributed below the depression at the origin of the frontal muscle; frons, aside from this area, with fewer than eight setae. Clypeus as depicted in Fig. 4D, E, with its width slightly exceeding than the minimum distance between the antennae. Main disc with a shallowly convex dorsal margin; dorsolateral corner angulate; lateral margins straight and weakly divergent ventrad, with tentorial pits but lacking pigmented spots; main disc relatively high, with a CLI of 3.0–5.0; main disc with approximately 75 setae; ventral section strongly transverse (Fig. 4E). Labrum (Fig. 4F, left) with numerous sensory bristles, except in the dorsal region. Palate (Fig. 4F, right) with a small median patch (width × height ≤ 0.02 × 0.02 mm), a large sclerotized patch extending nearly

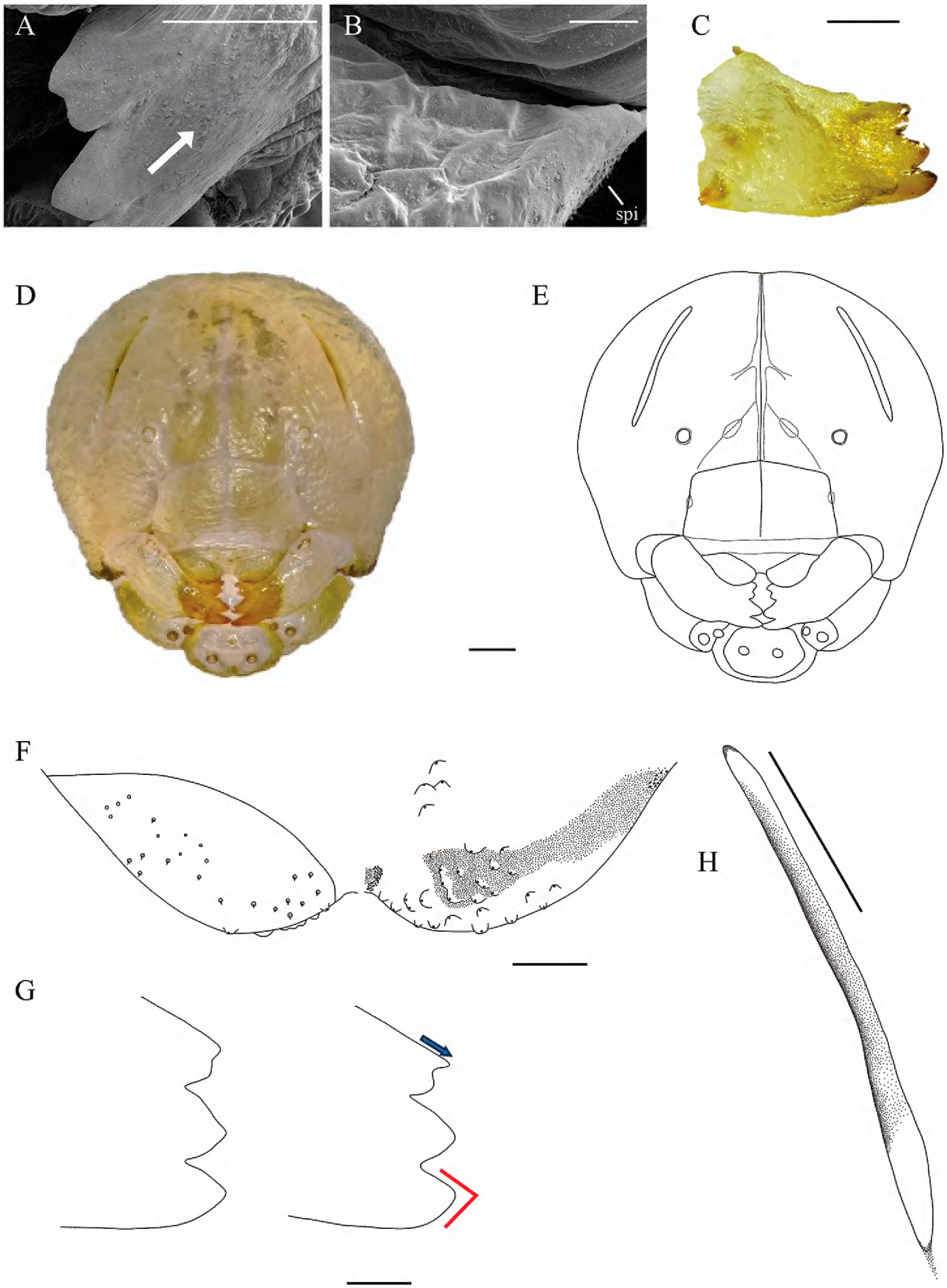

Figure 4. *Vespa ducalis* **A** left mandible in frontal view, with the arrow indicating pits **B** dorsolateral portion of the left half of the labrum in frontal view **C** right mandible **D, E** head in frontal view **F** labrum (left) and palate (right) in frontal view **G** two examples of the apical portion of the mandible, with the arrow showing the inclination of the dorsal margin of tooth III and red lines highlighting the acute apex of tooth I **H** temporal band. Scale bars: 0.2 mm (**A, C**); 0.03 mm (**B**); 0.3 mm (**D, E, H**); 0.1 mm (**F, G**).

to the dorsolateral extremity, and dense conical papillae concentrated medially, which become sparser laterad; largest conical papillae measuring 0.025 mm in basal width; spicules distributed in the medioventral region and along the ventrolateral margin (Fig. 4B, F). Mandible (Fig. 4A, C, G) slightly sclerotized (Fig. 4C), bearing numerous pits on its outer surface (Fig. 4A). Mandibular teeth I and II distinctly projected compared to IIIa and IIIb, with tooth I slightly more developed than tooth II, and tooth IIIa less produced than IIIb. Teeth I and II separated at an angle of 65°–85°, teeth II and IIIa separated at 60°–80°, and teeth IIIa and IIIb separated at 110°–160°. Teeth I and II stout, with triangular apices; tooth II with a slightly convex dorsal margin and a smooth, steep ventral margin. Teeth IIIa and IIIb directed downward; bifurcation point between teeth II and IIIa slightly deeper than other bifurcation points (Fig. 4G). Maxilla with approximately 30 setae. Prelabium with approximately 30 setae.

Body (thorax and abdomen): Body 21–34 mm in length (n = 47, mean 28.7 mm) and 10.5–12 mm in width (mean 11.0 mm); integument with sparse setae and dense spicules. Spiracles deep, generally similar in size, except for the slightly smaller spiracles 1, 2, and 10 (occasionally spiracles 2 and 10 smaller); largest spiracle 0.3 mm in diameter; spiracular rim 0.035 mm in thickness but rim of spiracle 2 relatively thick and consisting of sparse processes; inner part with short collar processes and thick, large, and even atrial processes; rim with short and sparse spicules.

Remarks. The cranium is orangish in color except in the area surrounding the antennae, a characteristic unique to *V. ducalis* (Fig. 4D). The dorsal (upper) region (main disc) of the clypeus is large and over three times the height of the ventral (lower) region (Fig. 4E). Mandibular tooth III is relatively small, measuring less than half as the length of tooth II (Fig. 4C, G).

Specimens examined. South Korea • 10 mature larvae; Gyeongsangbuk-do, Seongju-gun; 35°57'37"N, 128°10'56"E; 2 Aug. 2022; Ma • 10 mature larvae; Jeollanam-do, Gwangyang-si; 35°02'00"N, 127°37'21"E; 4 Aug. 2022 • 5 mature larvae; Gangwon-do, Wonju-si; 37°13'01"N, 128°05'18"E; 30 Aug. 2022; Ma and Kim • 42 mature larvae; Gyeongsangbuk-do, Chilgok-gun; 36°00'08"N, 128°27'33"E; 17 Aug. 2023; Choi and Kim • 5 mature larvae; Gyeongsandbuk-do, Andong-si; 36°33'41"N, 128°47'36"E; 18 Aug. 2023; Choi and Kim • 5 mature larvae; Gyeongsangbuk-do, Andong-si; 36°41'02"N, 128°49'39"E; 31 July 2024; Choi and Kim.

Vespa crabro flavofasciata Cameron, 1903

Description. ***Head*** (Fig. 5): CW/MW = 1.56–1.75 (n = 40, mean 1.66). Cranium with moderately strong, irregular rugo-reticulation, with the ventral area between the lateral margin of the clypeus and the outer margin of the cranium lacking this rugo-reticulation. Antenna positioned nearly at the level of the dorsal margin of the clypeus (Fig. 5E, F) with a distinctly sclerotized rim (Fig. 5E) and a diameter of 0.09 mm

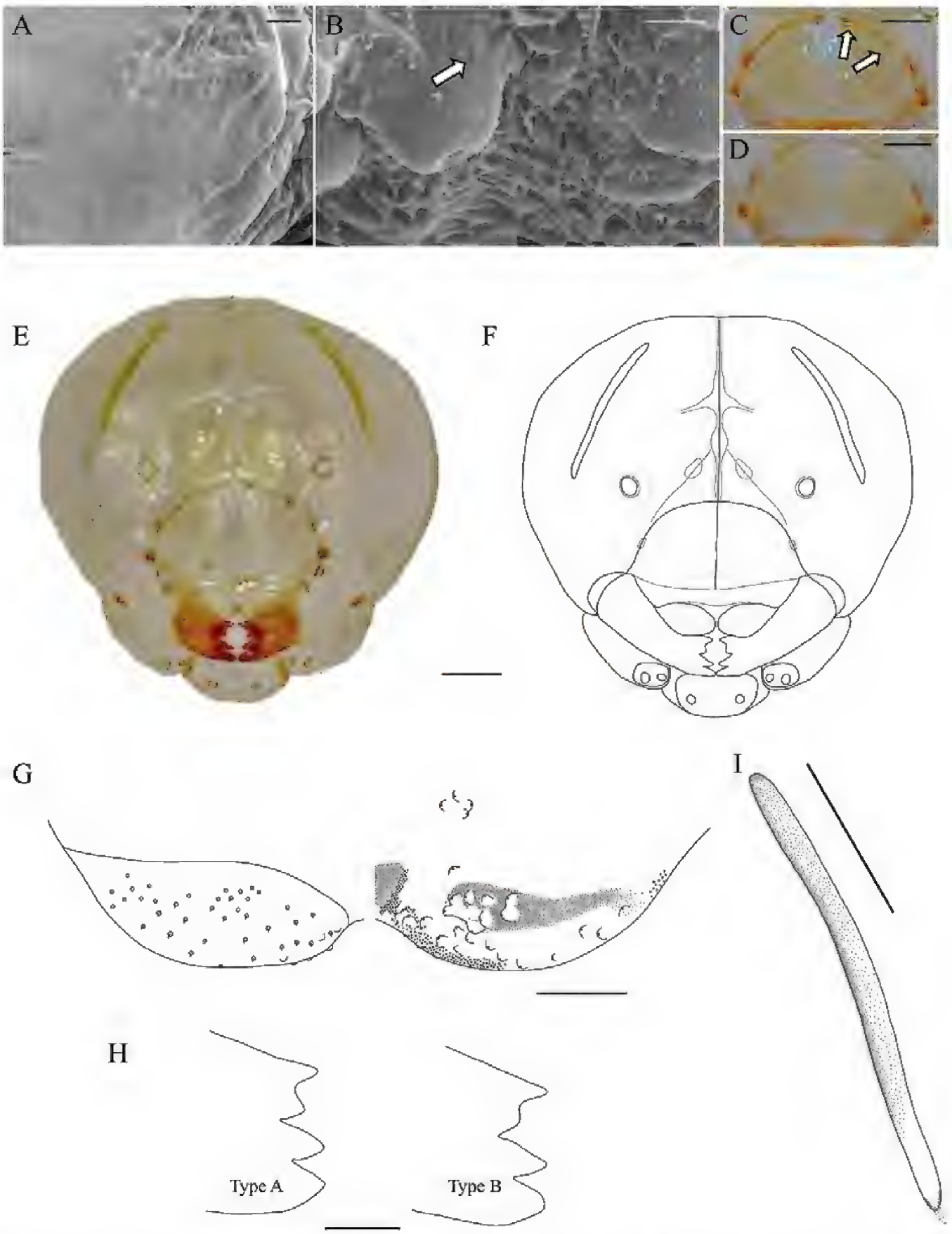

Figure 5. *Vespa crabro flavofasciata* **A** outer surface of the mandible **B** medioventral portion of the palate, showing minute spicules located on the conical papilla (indicated by an arrow) **C, D** clypeus in frontal view, highlighting pigmented spots on its dorsal and lateral margins **E, F** head in frontal view **G** labrum (left) and palate (right) in frontal view **H** two types of mandibular teeth. Scale bars: 0.03 mm (**A, B**); 0.3 mm (**C–F, I**); 0.1 mm (**G, H**)

(Fig. 5E, F). Temporal band (Fig. 5I) with moderately defined lateral margins and a heavily margined dorsal edge, with moderate ferruginous pigmentation in the inner area, except for the ventral one-fifth region; ventral extremity positioned lower than the dorsal margin of the antenna (Fig. 5F). Faint dotted patches on the frons, with

a few setae located around the frontal suture and fewer than 15 setae on other areas of the frons. Paired suprafrontal marks well defined (Fig. 5F). Clypeus width slightly exceeds the minimum distance between the antennae (Fig. 5F). Main disc with a broadly and roundly convex dorsal margin, merging with the lateral margin without separation from the latter; pigmented spots present along the margins except at the labroclypeal suture, with (Fig. 5C–E). Main disc relatively high, with a CLI of 1.5–3; main disc with approximately 80 setae; ventral section strongly transverse. Labrum (Fig. 5G, left) densely covered with small processes. Palate (Fig. 5G, right) with a large median patch; sclerotized patch dark, proximally wide, and narrowing distally, with conical papillae present in the proximal half; conical papillae also present in the ventral area of the palate; largest conical papillae 0.02 mm in diameter; spicules widely distributed in the medioventral region and dorsally along the lateral margin, and interspersed among the conical papillae (Fig. 5B). Mandible (Fig. 5A, E, H) with a heavily sclerotized apical third, with the entire surface containing numerous shallow pits (Fig. 5A). Mandibular teeth I and II distinctly projected in comparison to tooth III. Tooth I similar in size to or slightly more produced than tooth II, while IIIa similar to or smaller than IIIb; teeth I and II separated at an angle of 50°–70°, II and IIIa at 45°–80°, and IIIa and IIIb at 80°–105° (Type A) or 90°–135° (Type B, similar to the condition in *V. ducalis*); tooth I apically blunt and tooth II with a sharper apex (Type A); tooth II with a smooth dorsal margin and gibbous ventral margin; bifurcation point between teeth II and IIIa deeper than the other bifurcation points. Maxilla with 25–30 setae. Prelabium with approximately 25 setae.

Body (thorax and abdomen): Body 19.5–25 mm in length (n = 40, mean 21.5 mm) and 9–11 mm in width (mean 10.0 mm); integument with gradually increasing setae from the fifth integument posteriorly and with even spicules. Spiracles deep, generally uniform in size, except for spiracles 1, 2, and 10, which are slightly smaller; largest spiracle 0.3 mm in diameter; spiracular rim 0.03 mm in thickness, lacking any processes; collar processes thick and short (occasionally not thick).

Remarks. This species exhibits numerous dark spots along the dorsal and lateral margins of the clypeus. However, the number of spots varied among individuals. This variation may be due to certain environmental or genetic (Fig. 5C–E). The dorsal and lateral margins of the clypeus form a broad, rounded convex shape, creating an almost semi-circular arc, a characteristic observed only in *V. crabro flavofasciata* (Fig. 5C–E). In this species, mandibular tooth III presents in two forms (Fig. 5H): Type A is observed in most individuals, and Type B, observed in a few individuals, resembles the form observed in *V. ducalis*. For Type B mandibles, the angle between tooth IIIa and IIIb ranges from 90° to 135° (Fig. 5H). Additionally, spicules are distributed along the lateral margin of the palate, with a characteristic that contradicts the observations reported for *V. crabro* by Kojima (1998).

Specimens examined. South Korea • 10 mature larvae; Daegu; 35°59'27"N, 128°35'49"E; 27 July 2021; Choi and Kim • 10 mature larvae; Daegu; 35°53'31"N, 128°26'04"E; 28 July 2021; Choi and Kim • 10 mature larvae; Jeollanam-do, Naju-si; 35°01'46"N, 126°42'10"E; 18 Aug. 2021; Ma and Kim • 15 mature larvae; Gyeongsangbuk-do, Yecheon-gun; 36°40'16"N, 128°27'45"E; 2 Sept. 2022; Choi •

10 mature larvae; Gyeongsangbuk-do, Sangju-si; 36°21'58"N, 128°02'12"E; 5 July 2023; Choi and Ma • 30 mature larvae; Gyeongsangbuk-do, Andong-si; 36°35'12"N, 128°42'56"E; 18 Aug. 2023; Choi and Kim • 8 mature larvae; Gyeongsangbuk-do, Daegu; 35°54'59"N, 128°40'12"E; 20 Sept. 2023; Choi • 10 mature larvae; Gangwon-do, Hongcheon-gun; 37°47'19"N, 128°09'23"E; 22 Sept. 2023; Kim • 5 mature larvae; Gyeongsangnam-do, Gimhae-si; 35°21'36"N, 128°53'38"E; 10 Oct. 2023; Choi and Kim • 10 mature larvae; Gyeongsangbuk-do, Yecheon-si; 36°39'21"N, 128°24'10"E; 10 July 2024; Kim • 5 mature larvae; Gyeongsangbuk-do, Andong-si; 36°35'34"N, 128°46'35"E; 23 Oct. 2023; Choi and Kim.

Vespa analis parallela André, 1884

Description. ***Head*** (Fig. 6): CW/MW = 1.62–1.84 (n = 30, mean 1.71). Cranium with moderate, irregular rugo-reticulation. Antenna positioned well behind the level of the dorsal margin of the clypeus (Fig. 6C, D), with a diameter of 0.08 mm, rim thin yet strongly sclerotized. Temporal band (Fig. 6C, D, G) generally distinct, with relatively weakly defined edges and margins, except for the strongly margined and depressed dorsal edge; inner part moderately ferruginous-pigmented, except in the dorsal and ventral one-third portions; ventral edge positioned at the same level or slightly lower than the dorsal margin of the antenna. Dotted patches on the frons faint; region around the frontal suture and frons with setae in variable numbers. Paired suprafrontal marks relatively weak (Fig. 6D). Clypeus (Fig. 6C, D) with a maximum width similar to or slightly less than the minimum distance between the antennae; dorsal margin of the main disc shallowly convex; dorsolateral corner bluntly angulate; lateral margins slightly curved, diverging ventrad, and widest at the level of the interior mandibular articulation, lacking sclerotized pigmented spots, except in the tentorial pits; main disc not very high, with a CLI of 1.5–2; main disc with approximately 80 setae; ventral section distinctly transverse. Labrum (Fig. 6B, E, left), extensively covered with sensory bristles. Palate (Fig. E, right) with tiny median patch absent or present (width × height ≤ 0.02 × 0.02 mm) (Fig. 6E); sclerotized patch short and mostly faint, with a few conical papillae (up to 4) in the proximal area. Conical papillae aligned in line along the ventral margin; spicules widely and sparsely distributed in the medioventral area and along the lateral margin dorsally (Fig. 6B). Mandible (Fig. 6A, F) strongly sclerotized only in the extreme apical region, with numerous pits across the surface. Mandibular teeth smooth, sclerotized, and not strongly pronounced, with blunt apices (Fig. 6F); teeth I and II more produced than III; with tooth I slightly more produced than tooth II, with a significantly wider base; tooth IIIa less produced than IIIb; teeth I and II separated at an angle of 60°–80°, II and IIIa at 50°–80°, and IIIa and IIIb at 75°–105°; dorsal margin of tooth II slightly convex; bifurcation point between teeth II and IIIa relatively shallow, often shallower than other bifurcation points. Maxillar with approximately 25 setae (Sometimes lower than 15 setae). Prementeum with approximately 25 setae.

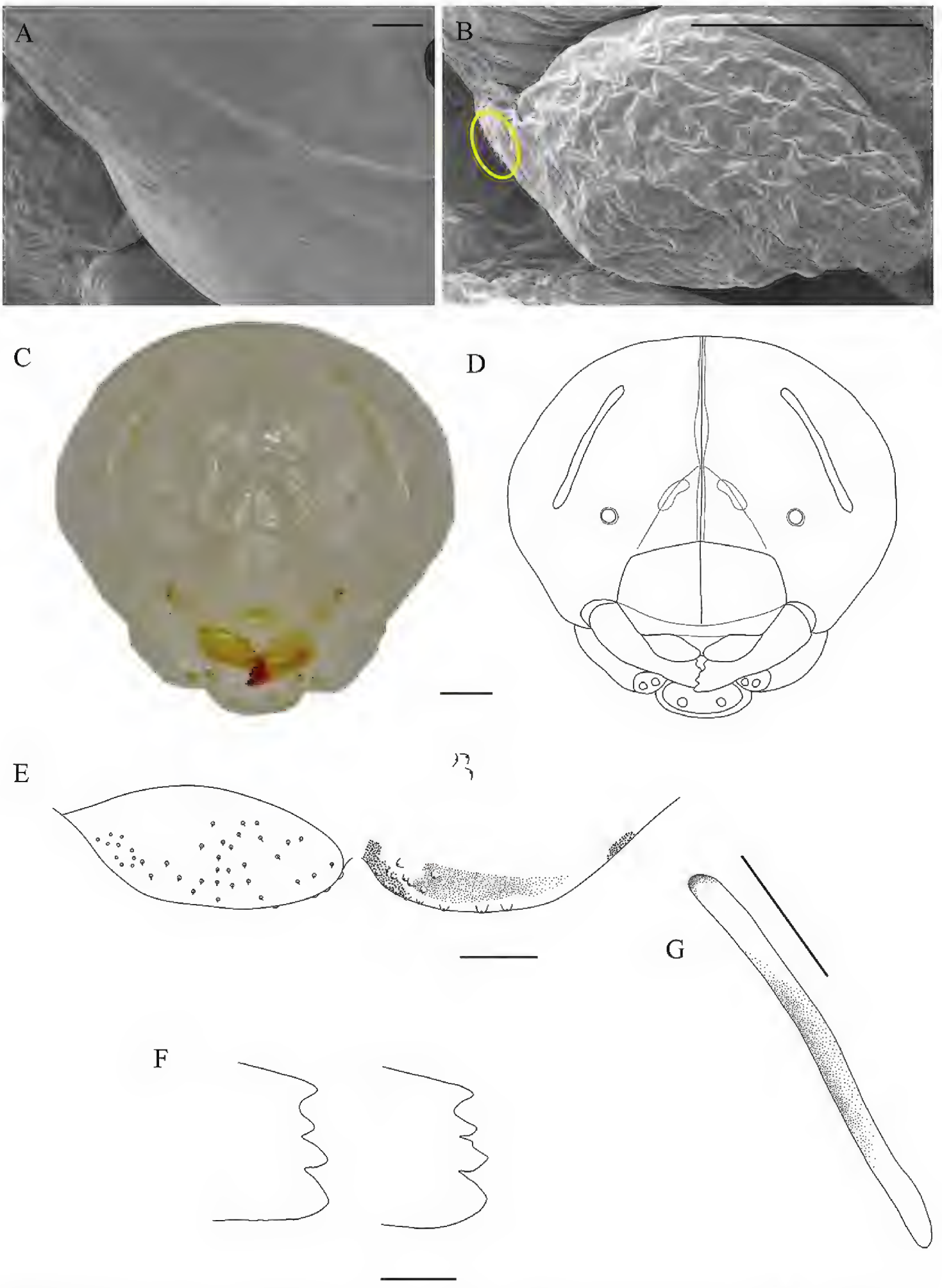

Figure 6. *Vespa analis parallela* **A** outer surface of the right mandible in frontal view **B** ventral portion of the palatolabral junction, with the yellow ring indicating the presence of spicules **C, D** head in frontal view **E** labrum (left) and palate (right) in frontal view **F** apical portion of the right mandible. Scale bars: 0.03 mm (**A**); 0.2 mm (**B**); 0.3 mm (**C, D, G**); 0.1 mm (**E, F**)

Body (thorax and abdomen): Body 22–27 mm in length (n = 30, mean 23.6 mm) and 10–11 mm in width (mean 10.7 mm); third, fourth, and fifth integuments with dense setae; spicules near spiracle 1 sparse and short. Largest spiracle 0.4 mm in diameter and shallow; approximately 0.7 times the size ratio of spiracles 1, 2, and 10, with sparse processes under 0.0025 mm in length on the inner edge; spiracular rim 0.04 mm in thickness with smaller and more sparse spicules on spiracles 1, 2, and 10.

Remarks. Similar to *V. velutina nigrithorax* and *V. simillima simillima*, this species has a relatively narrow clypeus, with a width comparable to or less than the minimum distance between the antennae, and lackse. However, unlike *V. velutina* and *V. simillima*, this species has abundant pits on the outer surface of the mandible.

Specimens examined. South Korea • 10 mature larvae; Gangwon-do, Gapyeong-gun; 37°50'45N, 127°30'44"E; 14 Sept. 2021; Choi • 10 mature larvae; Gyeongsangbuk-do, Gunwi-gun; 36°15'42"N, 128°30'36"E; 15 Sept. 2021; Choi and Ma • 5 mature larvae; Chungcheongbuk-do, Sejong-si; 36°33'39"N, 127°14'46"E; 19 July 2022; Choi and Ma • 7 mature larvae; Gyeongsangbuk-do, Seongju-gun; 36°00'18"N, 128°14'15"E; 5 Aug. 2022; Ma • 3 mature larvae; Daegu; 35°54'16"N, 128°42'46"E; 18 Oct. 2022; Ma • 10 Mature larvae; Gyeongsangnam-do, Goseong-si; 34°59'07"N, 128°08'34"E; 25 July 2023; Choi and Kim • 20 mature larvae; Daegu; 35°52'08"N, 128°31'35"E; 27 July 2023; Choi and Kim • 10 mature larvae; Gyeongsangbuk-do, Andong-si; 36°32'58"N, 128°48'11"E; 18 Aug. 2023; Choi and Kim • 15 mature larvae; Gyeongsangbuk-do, Pohang-si; 36°04'10"N, 129°09'44"E; 22 Aug. 2023; Choi and Ma • 20 mature larvae; Jeollabuk-do, Jeongeup-si; 35°34'45"N, 126°54'09"E; 17 Oct. 2024; Kim and Ma.

Vespa dybowskii André, 1884

Description. ***Head*** (Fig. 7): CW/MW = 1.55–1.75 (n = 30, mean 1.64). Cranium nearly circular in frontal view (Fig. 7B, C), with moderate irregular rugo-reticulation; rugo-reticulation absent in the ventral area of the cranium between the lateral margin of the clypeus and the outer margin of the cranium. Antenna positioned well behind the level of the dorsal margin of the clypeus (Fig. 7C), measuring 0.06–0.07 mm in diameter (Fig. 7B, C), with a heavily sclerotized rim. Paired suprafrontal marks well defined; dotted patches on the frons faint; area around the frontal suture with fewer than 10 widely distributed setae, with fewer than 10 setae on the frons. Temporal band (Fig. 7B, C, E) with heavily margined dorsal and ventral edges, with other parts exhibiting vaguely defined margins; inner region with moderate ferruginous pigmentation throughout; ventral edge positioned above the dorsal margin of the antenna (Fig. 7C). Clypeus as depicted in Fig. 7B, C; main disc with dorsal margin weakly convex, dorsolateral corner weakly angled, and lateral margin slightly curved and lacking pigmented spots, except in the tentorial pits; main disc not very high, with a CLI of 1.5–2; main disc with approximately 60 setae; ventral section with anterior margin shallowly concave medially. Labrum (Fig. 7D, left) with sensory bristles concentrated in the median half. Palate as shown in Fig. 7B, C, D (right); median patch and sclerotized patch

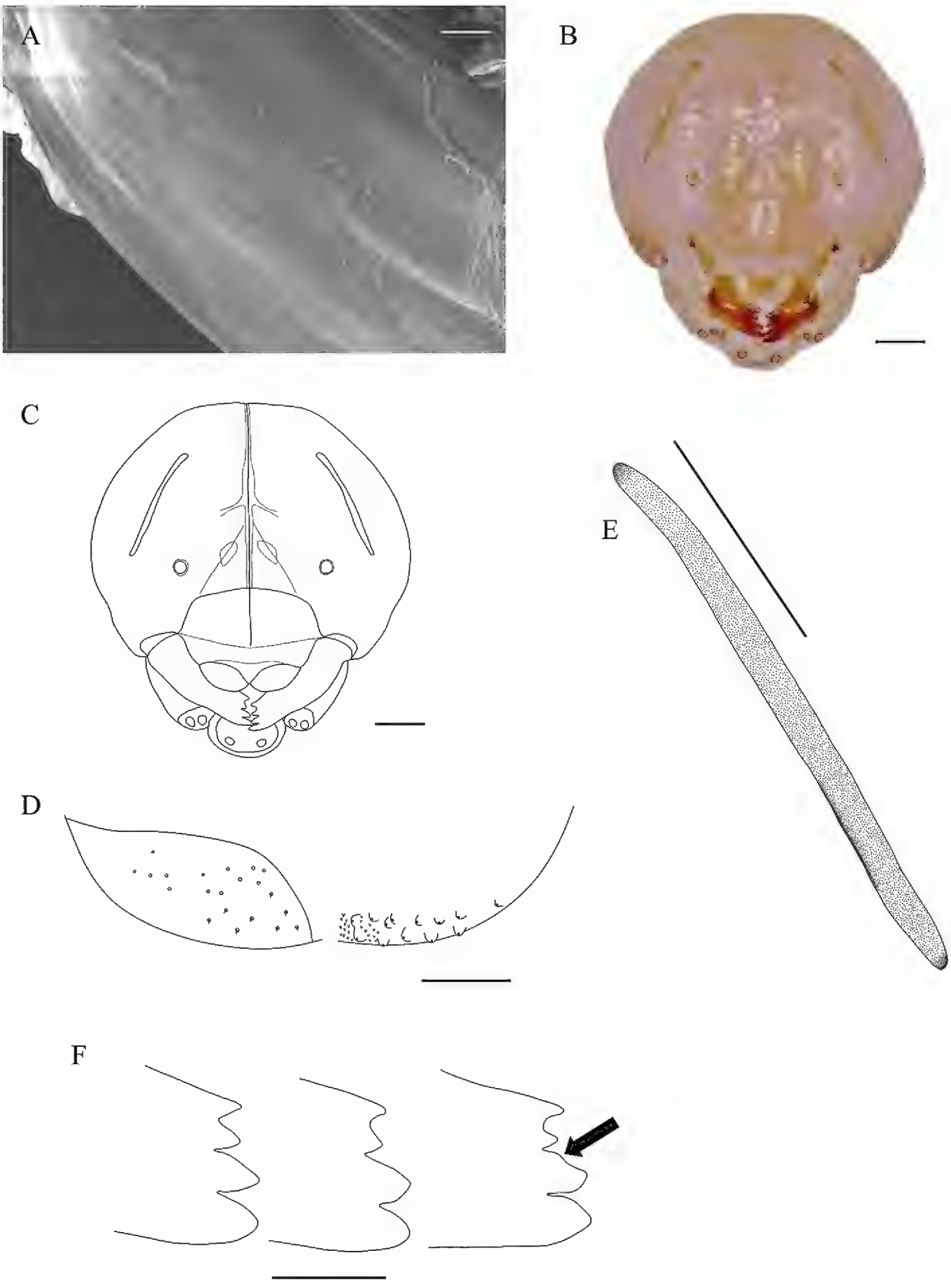

Figure 7. *Vespa dybowskii* **A** outer surface of the right mandible, showing the absence of pits on the outer surface **B, C** head in frontal view **D** labrum (left) and palate (right) in frontal view **E** temporal band **F** apical portion of the right mandible, with the arrow indicating a shallow incision on the dorsal margin of tooth II. Scale bars: 0.03 mm (**A**); 0.3 mm (**B, C, E**); 0.1 mm (**D, F**).

absent; conical papillae densely distributed ventrally and evenly dispersed; largest conical papilla measuring 0.025 mm in diameter at the base; most spicules located on the medioventral region. Mandible (Fig. 6B, F) with the apical half heavily sclerotized;

outer surface without pits but with a few bumps (Fig. 7A). Mandibular teeth I and II distinctly projected compared with tooth III; tooth I as large as II, and IIIa as large as IIIb; teeth I and II separated at an angle of 50°–80°, II and IIIa at 50°–80°, and IIIa and IIIb at 70°–105°; all teeth slick and relatively sharp at the apex, except for tooth II, which often has a faintly bifid dorsal margin; bifurcation point between teeth II and IIIa slightly deeper than other bifurcation points. Maxilla with approximately 20 setae. Prelabium with sparse setae.

Body (thorax and abdomen): Body 20–22 mm in length (n = 30, mean 21 mm) and 10–13 mm in width (mean 11.4 mm); integument with sparse setae. Spiracles shallow; generally uniform in size, except for spiracles 1, 2, and 10, which are slightly smaller; largest spiracle 0.3 mm in diameter, with a spiracular rim thickness of 0.025 mm, bearing dense processes.

Remarks. This species is distinguished by an entirely weakly pigmented temporal band and by having conical papillae and spicules confined to a narrow ventral zone on the palate.

Specimens examined. South Korea • 5 mature larvae; Jeollanam-do, Suncheon-si; 34°59'48"N, 127°24'54"E; 18 Aug. 2022; Choi and Ma • 9 mature larvae; Jeollanam-do, Gwangyang-si; 35°01'08"N, 127°39'28"E; 14 Oct. 2022; Choi and Ma • 11 mature larvae; Chungcheongbuk-do, Cheongju-si; 36°41'55"N, 127°39'19"E; 6 Sept. 2023; Choi and Kim • 20 mature larvae; Gyeongsangbuk-do, Andong-si; 36°38'01"N, 128°38'36"E; 01 Sept. 2023; Choi and Kim • 10 mature larvae; Gyeongsangbuk-do, Yeongyang-gun; 36°36'15"N, 129°04'31"E; 08 Sept. 2023; Choi et al. • 10 mature larvae; Gyeongsangbuk-do, Yeongyang-gun; 36°41'20"N, 129°08'48"E; 08 Sept. 2023; Choi et al. • 5 mature larvae; Gangwon-do, Bonghwa-gun; 36°58'35"N, 128°47'04"E; 19 Oct. 2022; Choi and Kim • 10 mature larvae; Gyeongsangbuk-do, Yeongyang-gun; 36°38'49"N, 129°09'24"E; 12 Sept. 2023; Kim.

Vespa simillima simillima Smith, 1868

Description. ***Head*** (Fig. 8): CW/MW = 1.61–1.87 (n = mean 1.7). Cranium with moderate irregular rugo-reticulation, with some areas exhibiting parallel reticulation. Antenna positioned near the level of the dorsal margin of the clypeus (Fig. 8D, E), faintly sclerotized or nearly transparent (Fig. 8D–F). Temporal band (Fig. 8F, G, J) with variable width; edges generally weakly margined except for the dorsal edge; inner part with moderate ferruginous pigmentation, excluding the dorsal and ventral regions; ventral edge positioned slightly above the dorsal margin of the antenna. Paired suprafrontal marks faint; dotted patches on the frons distinct, often extending ventrad (Fig. 8D, E); region distal to the frontal suture with 15–22 setae concentrated mainly around the base of the antenna; frons with fewer than 14 setae distributed medially. Clypeus (Fig. 8D–G) width similar to the minimum distance between the antennae; main disc with dorsal margin shallowly convex, dorsolateral corner roundly angulated, lateral margin slightly curved and lacking pigmented

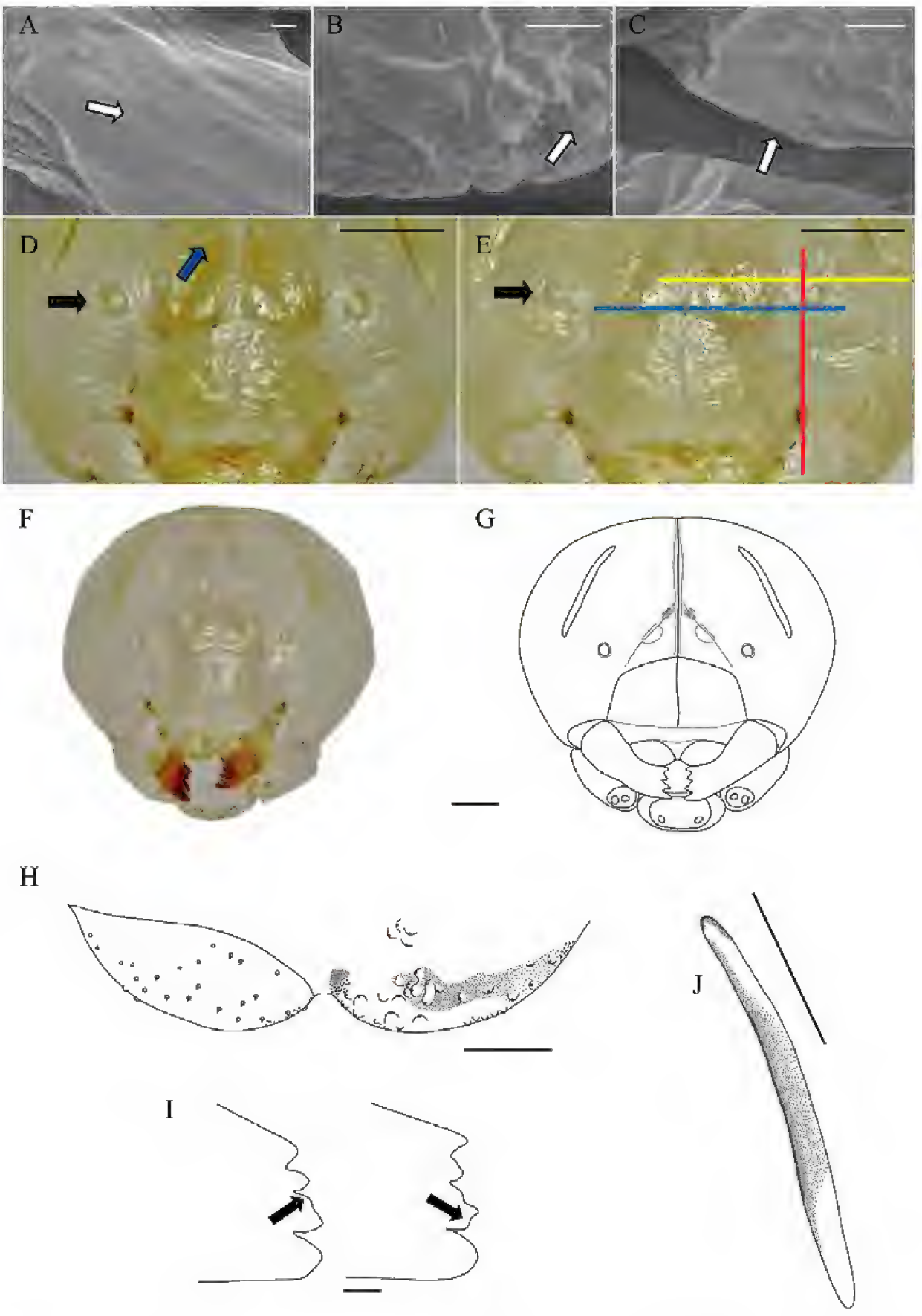

Figure 8. *Vespa simillima simillima* **A** basal portion of the right mandible, showing the absence of pits on the outer surface **B** minute spicules on the conical papillae (arrow) in the medioventral portion of the palate **C** spicules in the lateral part of the palatolabral junction **D, E** antenna and clypeus; black arrows indicate variations in antennal rim sclerotization, the blue arrow indicates a dotted patch on the frons, a blue line shows that the dorsalmost point of the clypeus and ventral margin of the antenna are at the same level, the red line is tangent to the inner margin of the antenna and the outermost point of the clypeus, and a yellow line showing the gap between the ventral margin of the temporal band and the dorsal margin of the antenna **F, G** head in frontal view **H** labrum (left) and palate (right) in frontal view **I** apical portion of the right mandible, with the arrow showing variation in the shape of tooth II **J** temporal band in *Vespa simillima* and *V. velutina*. Scale bars: 0.03 mm (**A–C**); 0.3 mm (**D–G, J**), 0.1 mm (**H, I**).

spots, except in the tentorial pits; ventral margin broadly convex; main disc not very high, with a CLI of 1.5–2; main disc with 45–60 setae; ventral section strongly narrowed dorsoventrally, with a straight ventral margin. Labrum (Fig. 8H, left) with numerous sensory bristles, except in the dorsolateral region. Palate (Fig. 8H, right) with a median patch; sclerotized patch reaching the apex of the palate, with variable pigmentation intensity; conical papillae small and dense ventrally, with over seven papillae located in the sclerotized patch, primarily medially (Fig. 8H); spicules present in the medioventral part and along the lateral margin of the palate, as well as on the conical papillae (Fig. 8C, H). Mandible (Fig. 8A, F, I) with strongly sclerotized teeth; surface lacking pits but bearing a few stumps (Fig. 8A). All mandibular teeth moderately produced and apically blunt; tooth I largest, stumpy, and round apically; tooth II often weakly bifid or trifid apically; tooth IIIa similar in size or slightly smaller than IIIb; teeth I and II separated at an angle of 55°–85°, II and IIIa at 65°–85°, and IIIa and IIIb at 65°–105°; bifurcation point between teeth II and IIIa slightly shallower than the other bifurcation points. Maxilla with approximately 30 setae. Prelabium with 45–50 setae.

Body (thorax and abdomen): Body 20.5–23.5 mm in length (n = 60, mean 22.2 mm) and 11–13 mm in width (mean 11.4 mm); integument with setae gradually decreasing in density posteriorly from the fifth integument (often evenly distributed across all segments); sparse spicules near the rim of spiracles 1 and 10 Spiracles shallow; generally uniform in size, except for spiracles 1, 2, and 10, which are slightly smaller; largest spiracle 0.3 mm in diameter; spiracular rim 0.03 mm in thickness, bearing sparse large processes (0.008–0.012 mm in length) and dense tiny processes (<0.01 mm in length).

Remarks. The antenna is typically nearly hyaline, as seen in *V. velutina* (Fig. 9D); however, it may be slightly sclerotized, as in *V. analis parallela* (Fig. 6C). This condition can vary even within a single colony. This species closely resembles *V. velutina* in both larval characteristics (Yamane 1976, present study) and adult features (Archer 1994; Carpenter et al. 2013).

Specimens examined. South Korea • 10 mature larvae; Chungcheongbuk-do, Goesan-gun; 36°48'42"N, 127°47'17"E; 29 Sept. 2022; Choi • 10 mature larvae; Gyeonsangbuk-do, Andong-si; 36°46'12"N, 128°47'48"E; 30 Sept. 2022; Ma • 30 mature larvae; Gyeongsangbuk-do, Yeongju-si; 36°50'09"N, 128°38'50"E; 12 Oct. 2022; Ma • 30 mature larvae; Gyeongsangbuk-do, Yeongyang-gun; 36°43'02"N, 129°05'48"E; 02 Aug. 2023; Choi and Kim • 5 mature larvae; Gyeonsangbuk-do, Yeongcheon-si; 36°04'00"N, 128°55'32"E; 5 Oct. 2023; Choi et al. • 5 mature larvae; Gyeonsangbuk-do, Yeongcheon-si; 36°04'05"N, 128°55'35"E; 5 Oct. 2023; Choi et al. • 10 mature larvae; Gyeonsangbuk-do, Yeongcheon-si; 36°03'35"N, 128°55'16"E; 5 Oct. 2023; Choi et al. • 10 mature larvae; Gangwon-do, Pyeongchang-si; 37°31'34"N, 128°30'08"E; 21 Aug. 2024; Ma and Kim • 15 mature larvae; Jeollanam-do, Gurye-gun; 35°14'40"N, 127°35'40"E; 22 Aug. 2024; Choi and Ma • 10 mature larvae; Gangwon-do, Hoengseong-gun; 37°31'31"N, 128°08'58"E; 5 Sept. 2024; Choi and Ma.

Vespa velutina nigrithorax du Buysson, 1905

Description. ***Head*** (Fig. 9): CW/MW = 1.64–1.76 (n = 1.68). Cranium with moderate, irregular rugo-reticulation, except for some parallel rugae between the temporal band and the mid-cranial sulcus. Antenna positioned near the level of the dorsal margin of the clypeus (Fig. 9D, E), measuring 0.08–0.1 mm in diameter (Fig. 9E), with very weak pigmentation and a hyaline antennal socket (Fig. 9D). Temporal band (Fig. 9D, E) similar to that in *V. simillima* (Fig. 8J), with variation in width; edges mostly weakly margined; inner part with moderate ferruginous pigmentation in the dorsal and ventral areas or mostly transparent; ventral edge positioned above the dorsal margin of the antenna. Paired suprafrontal marks relatively weak; dotted patches on the upper frontal area distinct and extending ventrad (Fig. 9D, E: arrow); region around the frontal suture with 18–23 setae, primarily in the dorsal area; frons, except for this region, with fewer than 14 setae distributed between the *dfm* and the clypeus. Clypeus (Fig. 9D, E) with a width similar to or less than the minimum distance between the antennae; dorsal margin of the main disc roundly convex; lateral margin slightly curved, without pigmented spots, except in the tentorial pit; ventral margin shallowly convex; main disc not very high, with a CLI of 1.5–2; main disc with 40–50 setae (sometimes lower than 60 setae); ventral section strongly transverse, with a straight anterior margin. Labrum (Fig. 9F, left) bearing numerous sensory bristles, except in the zone along the dorsal margin. Palate (Fig. 8B, C, F: right) with a small median patch (0.03 × 0.03 mm); sclerotized patch relatively poorly developed and pale in color, not extending to the dorsolateral part; conical papillae tiny and densely arranged ventrally; with fewer than 10 papillae present on the sclerotized patch; spicules distributed in the medioventral part, along the lateral margin of the palate, and on the conical papillae (Fig. 9C, F). Mandible (Fig. 9D, E, G) strongly sclerotized in the apical two-fifths; outer surface without pits but with a few bumps (Fig. 9A) or extensively smooth. All mandibular teeth smooth and moderately produced (Fig. 9G); tooth I similar in size to, or slightly larger and more produced than, tooth II, occasionally bearing small denticles on the dorsal margin; tooth IIIa similar to or more produced than IIIb; teeth I and II separated at an angle of 65°–90°, II and IIIa at 60°–90°, and IIIa and IIIb at 75°–105°; bifurcation point between teeth II and IIIa slightly deeper than the other bifurcation points. Maxilla with approximately 25 setae. Prelabium with approximately 45–55 setae.

Body (thorax and abdomen): Body 21–23.2 mm in length (n = 50, mean 21.8 mm) and 10–12 mm in width (mean 11.1 mm); integument with setae gradually decreasing in density posteriorly from the fifth integument (often evenly distributed across all segments) with dense spicules. Spiracle shallow; generally uniform in size, except for spiracles 1, 2, and 10, which are slightly smaller; largest spiracle 0.3 mm in diameter; spiracular rim 0.03 mm in thickness with dense spicules of variable sizes.

Remarks. Mature larvae exhibit minimal variation within a single colony and consistently retain traits comparable to those of *V. simillima simillima*. However, distinguishing them from some individuals of *V. simillima simillima* based solely on morphology is challenging.

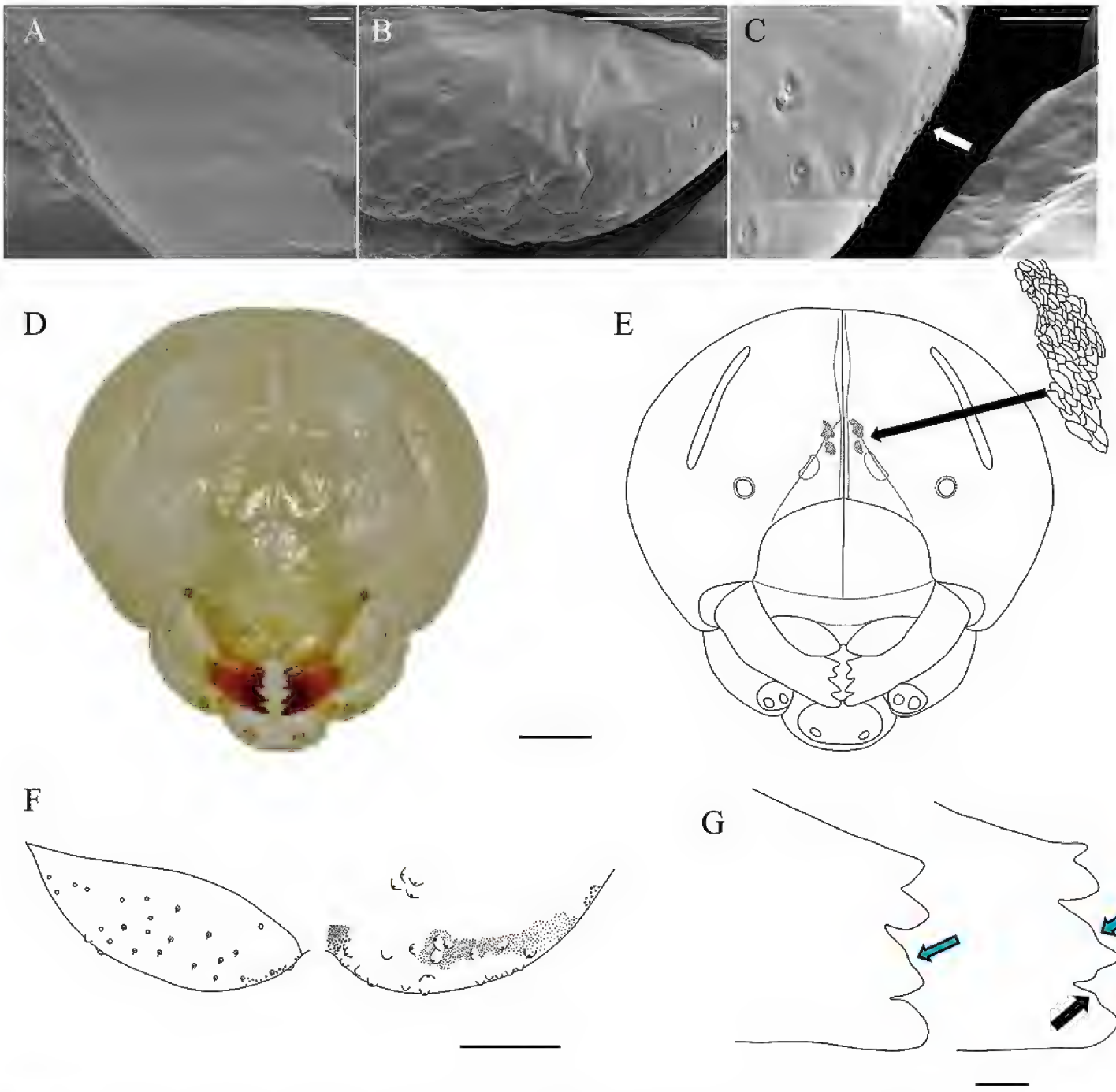

Figure 9. *Vespa velutina nigrithorax* **A** basal area of the right mandible, showing the absence of pits **B** left half of the labrum in ventrofrontal view **C** lateral part of the labrum showing spicules on the palate (arrow) **D, E** head in frontal view, with the arrow indicating a dotted patch (*dt*) and an enlarged image **F** labrum (left) and palate (right) in frontal view **G** apical portion of the right mandible, with the arrow showing variations in the shape of teeth I and II. Scale bars: 0.03 mm (**A, C**); 0.1mm (**B, F, G**); 0.3 mm (**D, E**).

Specimens examined. South Korea • 30 mature larvae; Jeonllanam-do, Guryegun; 35°25'57"N, 127°58'62"E; 10 Sept. 2021; Choi • 10 mature larvae; Gyeonggi-do, Pocheon-si; 37°58'36"N, 127°14'24"E; 13 Oct. 2022; Choi and Ma • 10 mature larvae; Gyeongsangnam-do, Sacheon-si; 35°01'37"N, 128°07'20"E; 19 Oct. 2022; Choi and Ma • 20 mature larvae; Daegu; 35°48'40"N, 128°33'07"E; 7 Sept. 2023; Choi et al. • 5 mature larvae; Gyeongsangbuk-do, Cheongdo-gun; 35°40'37"N, 128°43'19"E; 17 Oct. 2023; Choi and Kim • 5 mature larvae; Chungcheongbuk-do, Boeun-gun; 36°26'28"N, 127°41'35"E; 15 July 2024; Choi • 15 mature larvae; Gyeongsangbuk-do, Gyeongsan-si; 35°49'07"N, 128°43'14"E; 13 Aug. 2024; Ma and Kim • 10 mature larvae; Jeollabuk-do, Muju-gun; 35°52'13"N, 127°39'12"E; 19 Sept. 2024; Ma • 15 mature larvae; Gyeongsangbuk-do, Andong-si; 36°34'05"N, 128°43'33"E; 24 Sept. 2024; Ma

and Kim • 15 mature larvae; Gyeongsangbuk-do, Andong-si; 36°33'54"N, 128°43'27"E; 25 Sept. 2024; Ma • 20 mature larvae; Gyeongsangbuk-do, Gyeongsangbuk-do, Andong-si; 36°56'80"N, 128°70'57"E; 02 Sept. 2023; Choi and Kim.

Vespa binghami du Buysson, 1905

Description. ***Head*** (Fig. 10): CW/MW = 1.56–1.68 (n = 10, mean 1.63). Cranium with moderate, irregular rugo-reticulation. Antenna positioned well behind the dorsal margin of the clypeus (Fig. 10D), with a diameter of 0.1 mm and a thin but heavily sclerotized rim (Fig. 10C). Temporal band (Fig. 10C, D, G) relatively broad, with its ventral half wider than the dorsal half; edges heavily margined; inner part with heavy ferruginous pigmentation, except for the ventral one-third portion, which is nearly transparent. Paired suprafrontal marks well defined (Fig. 10D); dotted patches on the frons faint; region around the frontal suture with 12 or 14 setae. Clypeus width larger than the minimum distance between the antennae. Clypeus as shown in Fig. 10C, D; main disc with dorsal margin convex, with lateral arms straight, and dorsolateral corner roundly angulate; lateral margin straight and lacking pigmented spots, except in the tentorial pit; ventral margin shallowly convex; main disc moderately high, with a CLI of 1.5–2.5; main disc with approximately 85 setae; ventral section strongly transverse, with dorsal and ventral margins nearly parallel. Labrum (Fig. 10E, left) with numerous sensory bristles widely distributed across its surface. Palate (Fig. 10E, right) without a median patch; sclerotized patch relatively poorly developed; conical papillae dense in the proximal half of the sclerotized patch and sparser distally; spicules distributed in the medioventral part of the palate (Fig. 10B, E). Mandible heavily sclerotized in the apical two-fifth portion (Fig. 10C), with numerous pits on the outer surface (Fig. 10A). Mandibular teeth (Fig. 10F) all smooth with relatively sharp apices; teeth I and II significantly more projected than IIIa and IIIb; tooth I as large as II; tooth IIIb slightly more produced than IIIa; teeth I and II separated at an angle of 50°–60°, II and IIIa at 60°–70°, and IIIa and IIIb at 90°–140°; tooth I triangular and raised basally; bifurcation point between teeth II and IIIa deeper than the other bifurcation points. Maxilla with approximately 25 setae. Prelabium with 25–35 setae.

Body (thorax and abdomen): Body 29.8–31.4 mm in length (n = 10, mean 30.6 mm) and 12 mm in width; integument with evenly distributed setae; sparse and short spicules near the rim of spiracles 1 and 10. Spiracles shallow; generally uniform in size, except for spiracles 1, 2, and 10, which are slightly smaller; largest spiracle 0.35 mm in diameter; inner wall of spiracle with dense, long atrial processes; collar processes thick; spiracular rim 0.04 mm in thickness.

Remarks. As in *V. ducalis*, mandibular teeth I and II are strongly developed. The temporal band, antennal rim, and mandible are more heavily pigmented compared to those in other species.

Specimens examined. South Korea • 10 mature larvae; Gyeongsangbuk-do, Andong-si, Namhu-myeon; 36°52'99"N, 128°67'48"E; 2 Sept. 2022; Choi.

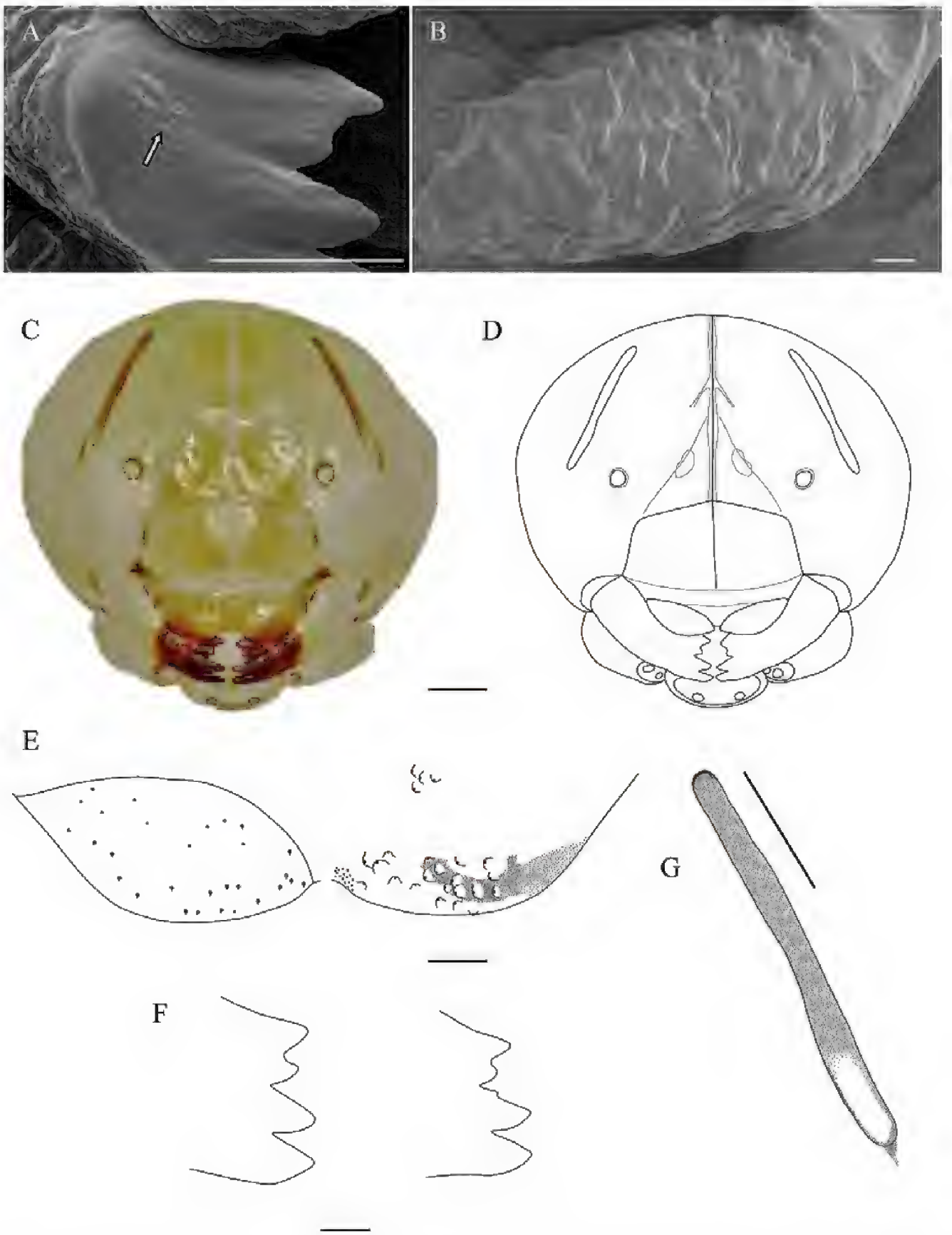

Figure 10. *Vespa binghami* **A** right mandible, with the arrow indicating pits **B** labrum in ventrofrontal view **C, D** head in frontal view **E** labrum (left) and palate (right) in frontal view **F** apical portion of the right mandible **G** temporal band. Scale bars: 0.1 mm (**A, E, F**); 0.03 mm (**B**); 0.3 mm (**C, D, G**).

Identification key for mature larvae of Korean *Vespa* species

1 Clypeus width larger than the minimum distance between the antennae (Fig. 3G) **2**

– Clypeus width similar to or smaller than the minimum distance between the antennae (Fig. 8E) **6**

2 Ventral margin of the temporal band positioned above the level of the dorsal margin of the antenna (Fig. 3G) **3**

– Ventral margin of the temporal band positioned below the level of the dorsal margin of the antenna (Figs 6C, 10C) **5**

3 Sclerotized patch present on the palate (Fig. 3F) **4**

– No sclerotized patch on the palate (Fig. 7D) ..... ***V. dybowskii***

4 CW/MW < 1.5. Main disc of the clypeus not elevated, with a CLI < 2 (Fig. 3D, E) ..... ***V. mandarinia***

– CW/MW > 1.6. Main disc of the clypeus more elevated, with a CLI > 3 (Fig. 4D, E) ..... ***V. ducalis***

5 Dorsal margin of the clypeus continuous with the lateral margin without a distinct dorsolateral angle, forming a semi-circular arc with several pigmented spots (Fig. 5C–F) ..... ***V. crabro flavofasciata***

– Dorsal margin of the clypeus convex, separated from the lateral margin with the dorsolateral corner more or less roundly angulate; dorsal and lateral margins without pigmented spots (Fig. 10C, D) ..... ***V. binghami***

6 Mandible without pits on the outer surface (Figs 8A, 9A); sclerotized patch on the palate with more than four conical papillae (Figs 8H, 9F) 7

– Mandible with pits on the outer surface (Fig. 6A); sclerotized patch on the palate with fewer than four conical papillae (Fig. 6E) ..... ***V. analis parallela***

7 Antennal rim not distinctly sclerotized, appearing almost entirely transparent (Fig. 9D); dotted patches distinct and extending ventrad (Fig. 9E) ..... ***V. velutina nigrithorax***

– Antennal rim faintly sclerotized or nearly transparent, with variations observed within a colony (Fig. 8D–F); dotted patches distinct and sometimes extended ventrad, with variations observed within a colony ..... ***V. simillima simillima***

Discussion

Compared to adults, vespine larvae exhibit limited morphological differences across species, making taxonomic classification challenging. Conversely, polistine larvae exhibit more distinct morphological variations in certain characteristics, such as the size and distribution of hairs and bristles, which facilitate chaetotaxy-based analyses (Yamane and Okazawa 1981; Kojima and Yamane 1984; Kojima 1998). Chaetotaxy is frequently employed in phylogenetic studies of other insect larvae, particularly in Coleoptera and Lepidoptera (Solodovnikov 2007; Komai et al. 2011; Michat et al. 2016). In the genus *Vespa*, the number of setae on the clypeus of *V. simillima simillima* and *V. velutina nigrithorax* was observed to be significantly lower compared to other species. Additionally, the spicules on the body integument were noticeably denser in these species. Furthermore, slight interspecific differences in spicule density were observed around the rims of certain spiracles. Although vespine larvae may exhibit some species-specific tenden-

cies in chaetotaxic patterns, these patterns are generally insufficient for similar species, *V. simillima simillima* and *V. velutina nigrithorax*, identification.

Certain species among the hornet fauna of Korea and Japan can be more readily distinguished based on larval characteristics. For instance, *V. mandarinia* exhibits the smallest cranial-to-mouthparts width ratio (CW/MW: 1.29–1.42, mean 1.39), whereas all other species have a CW/MW greater than 1.55 (see also Yamane 1976). *V. crabro flavofasciata* is unique in possessing several dark spots along the lateral margin of the clypeus. The dorsal and lateral margins of the clypeus are continuous, lacking a distinct dorsolateral corner and forming a smooth semicircular arch. These characteristics were not noted by Reid (1942) and Kojima (1998) in their examination of British and Japanese specimens of this species. Yamane (1976) classified this species within the *V. velutina* group; however, the present study disagrees with this classification. A weakly pigmented temporal band distinguishes *V. dybowskii* from other Korean species. Additionally, the absence of a median patch on the palate aids in identifying this species; the median patch is also absent in *V. binghami* and may be absent in *V. mandarinia* and *V. analis parallela* (see below). The present study found significant differences in the distribution of the sclerotized patch, conical papillae, and spicules on the palate of *V. dybowskii* compared to the findings of Kojima (1998). It remains unclear whether these differences result from local variation or observational errors. *V. ducalis* can be identified by the distinctive orangish coloration of its cranium, a trait specific to this species. *V. binghami* has distinctly thicker collar processes on the spiracles compared to other species. It shares similarities with *V. crabro flavofasciata* but exhibits significant differences in the thickness of the temporal band and the shape of the clypeus margin (Figs 9, 10).

The species observed in Kojima (1998) showed a well-defined distribution of setae and spicules on the cranium, mouthparts, and body integument. In this study, the analysis of the cranium particularly focused on structural aspects beyond chaetotaxy, as quantifying the spicules on the cranium in a stable manner is challenging. According to Kojima (1998), *V. analis parallela* typically has approximately 40 setae on the maxilla, with some individuals in certain regions bearing approximately 25 setae. Our observations showed that most individuals had approximately 25 setae, while some had fewer than 15. Additionally, it was confirmed that in most species, the first spiracle (and occasionally the second) and the last spiracle were slightly smaller than the others, partially aligns with the observations in the report by Kojima (1998). In this study, the mandibular teeth of *V. simillima simillima* and *V. analis parallela* were categorized under the same type, characterized by the separation of teeth IIIa and IIIb and their distinctly smaller size compared to teeth I and II. The differences between these two groups are also distinguishable in figs 1187, 1202, and 1214 in the report by Kojima (1998). *V. affinis* Linnaeus, 1764, which is not found in South Korea and was not included in this study, exhibits significant mandibular shape similarities (fig. 1179 in Kojima 1998) with *V. ducalis*. However, as these two species are phylogenetically distant (Perrard et al. 2015), this similarity is unlikely to have phylogenetic significance. *V. crabro flavofasciata* is distributed in both South Korea and Japan, and the specimens examined in this study are the same species as those investigated by Kojima (1998). According to Kojima (1998), the mandibular

shape of *V. crabro flavofasciata* in Japan was characterized by an overwhelmingly small tooth IIIa. However, in this study, some specimens did not exhibit this trait. Therefore, their mandibular shape was classified into two distinct types (Fig. 5). Among the species examined by Kojima (1998), most comparable specimens were collected from Japan, making it difficult to overlook certain differences between the two studies. Given that similar variations were observed across different regions in South Korea, it is likely that these variations arose either due to geographical divergence between the Japanese and Korean populations or as a result of mosaic traits inherent to larvae of the genus *Vespa*.

In this study, we introduce a morphological feature not previously noted by other authors: the paired suprafrontal marks, which appear to branch from the median cranial sulcus just above the frons (Fig. 3E). This structure is observed in species other than *V. analis parallela*, *V. simillima simillima*, and *V. velutina nigrithorax* (see above). The function and phylogenetic significance of this feature remains unknown. Another previously overlooked characteristic that differentiates species is the relative position (or configuration) of the temporal band and the antenna (refer to the key to species, couplet 2). The presence or absence of a median patch, the condition of the temporal band margins, and the relative sizes of mandibular teeth IIIa and IIIb have been considered useful for distinguishing Japanese and Taiwanese hornet species (Yamane 1976). Although the median patch was previously considered a key characteristic for differentiating *V. simillima simillima*, *V. velutina nigrithorax*, and *V. analis parallela* from other species (Yamane 1976), this study also observed it in *V. mandarinia* (Fig. 3C, F) and *V. ducalis* (Fig. 4F). Intraspecific variation in this feature was noted in these two species, raising questions about the reliability of this trait for species identification.

The mature larva of *V. analis parallela* shares certain morphological similarities with *V. simillima simillima* and *V. velutina nigrithorax* (Yamane 1976, present study), particularly the absence of paired suprafrontal marks, which may represent an important distinguishing feature. However, in *V. simillima simillima* and *V. velutina nigrithorax*, the median patch on the palate is always distinct, the mandible lacks pits on its outer surface, and the mandible is more extensively and strongly sclerotized compared to *V. analis parallela*. Carpenter et al. (2013) also placed *V. analis* in a clade distant from the one that includes *V. simillima* and *V. velutina*. These three species also exhibit similar nesting habits, constructing aerial nests covered by a complete envelope when built in open sites (Matsuura and Yamane 1990). It remains unclear whether the similarities in larval characteristics among these species are related to their nesting habits. Nonetheless, the close relationship between *V. simillima simillima* and *V. velutina nigrithorax* is supported by both adult and larval morphology, as well as molecular data (Archer 1993; Carpenter et al. 2013; Perrard et al. 2016).

In terms of adult morphology, *Vespa* species are relatively homogeneous, particularly with regard to structural characteristics (Yamane 1976; Carpenter et al. 2013). However, these species often exhibit significant differences in body coloration and behavior, facilitating species identification for adults within local faunas, despite occurrences of regional convergence in body marking patterns (van der Vecht 1957). In contrast, distinguishing species in the larval stage is more challenging owing to their

simpler yet highly variable structure. In many social Hymenoptera, nests are protected from external environmental conditions by being constructed in concealed sites or by being enclosed within a thick covering (Spradbery 1973; London and Janne 1998; Wenzel 2020). Particularly in vespine species, genetic changes affecting larval phenotypes may have been minimal throughout their evolutionary history, given the stable and protected conditions within the nest (Wheeler and Wheeler 1976). These constant and homogeneous nesting conditions likely exerted little selective pressure for morphological divergence among larvae, thereby enhancing their survival rates. As a result, any morphological differences observed in hornet larvae may be relatively subtle. Although the present study shows that establishing species groups based solely on larval characteristics remains a challenging task, these characteristics could have significant implications for understanding their phylogeny.

Acknowledgments

This work was supported by a grant from the National Research Foundation of Korea (NRF), funded by the Korean government (MSIT) (No. RS-2023-00212908). It is based on a research paper that was submitted to and awarded at the "2023 Undergraduate Student Biological Taxonomy Research Paper Contest," hosted by the National Institute of Biological Resources (NIBR), Korea. We also thank Prof. Jongok Lim (Wonkwang University) for his advice on character analysis, Prof. Seungyeol Lee (Kyungpook National University) for his guidance on SEM imaging, and Mr. Ma for his assistance in collecting hornet colonies.

References

Abe T, Tanaka Y, Miyazaki H, Kawasaki YY (1991) Comparative study of the composition of hornet larval saliva, its effect on behaviour and role of trophallaxis. Comparative Biochemistry and Physiology Part C 99(1–2): 79–84. https://doi.org/10.1016/0742-8413(91)90079-9

Archer ME (1993) A phylogenetic study of the species of the genus *Vespa* (Hymenoptera: Vespinae). Insect Systematics & Evolution 24(4): 469–478. https://doi.org/10.1163/187631293X00226

Archer ME (1994) Taxonomy, distribution, and nesting biology of the *Vespa bicolor* group (Hym., Vespinae). Entomologist's Monthly Magazine 130: 149–158. https://www.cabidigitallibrary.org/doi/full/10.5555/19951100676

Carpenter J, Kojima J, Villemant C (2013) Phylogeny of hornets: a total evidence approach (Hymenoptera, Vespidae, Vespinae, *Vespa*). Journal of Hymenoptera Research 32: 1–15. https://doi.org/10.3897/jhr.32.4685

Choi MB (2021) Defensive behavior of the invasive alien hornet *Vespa velutina nigrithorax* against potential human aggressors. Journal of Entomological Research 51(4): 186–195. https://doi.org/10.1111/1748-5967.12514

Choi MB, Kim JK, Kwon O (2019) Recent trends in wasp nest removal and Hymenoptera stings in South Korea. Journal of Medical Entomology 56(1): 254–260. https://doi.org/10.1093/jme/tjy144

Choi MB, Kim JK, Lee JW (2012) Increase trend of social hymenoptera (wasps and honeybees) in urban areas, inferred from moving-out case by 119 rescue services in Seoul of South Korea. Journal of Entomological Research 42(6): 308–319. https://doi.org/10.1111/j.1748-5967.2012.00472.x

Choi MB, Kim JK, Lee JW (2013) Checklist and distribution of Korean Vespidae revisited. Journal of Applied Entomology 52(2): 85–91. https://doi.org/10.5656/KSAE.2013.02.1.072

Fleck G, Brenk M, Misof B (2008) Larval and molecular characters help to solve phylogenetic puzzles in the highly diverse dragonfly family Libellulidae (Insecta: Odonata: Anisoptera): the Tetrathemistinae are a polyphyletic group. Organisms Diversity & Evolution 8(1): 1–16. https://doi.org/10.1016/j.ode.2006.08.003

Jeyanthi KG (2010) Fatality by multiple Asian giant hornet stings: Two case reports from south India. Journal of South India Medicolegal Association 2(2): 68–71.

Kim JK, Choi M, Moon TY (2006) Occurrence of *Vespa velutina* Lepeletier from Korea, and a revised key for Korean *Vespa* species (Hymenoptera: Vespidae). Journal of Entomological Research 36(2): 112–115. https://doi.org/10.1111/j.1748-5967.2006.00018.x

Kojima J (1998) Larvae of social wasps (Insecta: Hymenoptera: Vespidae). Natural History Bulletin of Ibaraki University 2: 7–227.

Kojima J, Hartini S, Noerdjito WA, Kahono S, Fujiyama N, Katakura H (2001) Descriptions of pre-emergence nests and mature larvae of *Vespa fervida*, with a note on a multiple foundress colony of *V. affinis* in Sulawesi (Hymenoptera: Vespidae; Vespinae). Entomological Science 3: 355–360. http://dl.ndl.go.jp/info:ndljp/pid/10656455

Kojima J, Yamane Sk (1984) Systematic study of the mature larvae of oriental Polistine wasps (Hymenoptera: Vespidae) (1) Species of *Ropalidia* and *Polistes* from Sumatra and Java Islands. Reports of the Faculty of Science, Kagoshima University (Earth Science & Biology) 17: 103–127. http://hdl.handle.net/10232/5951

Komai F, Yoshiyasu Y, Nasu Y, Saito T (2011) A Guide to the Lepidoptera of Japan. Kanagawa: Tokai University Press, 1305 pp.

Landaverde R, Rumble J (2020) Fear or preparedness? A Content Analysis of the "Murder Hornet" News in the United States; 2020 Aug; Annual Conference of the American Association for Agricultural Education – North Central Region, Columbus, Ohio: The Ohio State University.

Lima CG, Vaz AS, Honrado JP, Aranha J, Crespo N, Vicente JR (2022) The invasion by the Yellow-legged hornet: A systematic review. Journal of Nature Conservation 67: 126173. https://doi.org/10.1016/j.jnc.2022.126173

Lioy S, Bergamino C, Porporato M (2022) The invasive hornet *Vespa velutina*: Distribution, impacts and management options. CABI Reviews 2022: 11. https://doi.org/10.1079/cabireviews202217030

London KB, Jeanne RL (1998) Envelopes protect social wasps' nests from phorid infestation (Hymenoptera: Vespidae, Diptera: Phoridae). Journal of the Kansas Entomological Society 175–182. https://www.jstor.org/stable/25085830

Marvaldi AE (1997) Higher level phylogeny of Curculionidae (Coleoptera: Curculionoidea) based mainly on larval characters, with special reference to broad-nosed weevils. Cladistics 13(4): 285–312. https://doi.org/10.1111/j.1096-0031.1997.tb00321.x

Matsuura M, Yamane Sk (1990) Biology of the vespine wasps, English edition. Berlin: Springer-Verlag. https://doi.org/10.1007/978-3-642-75230-8

Michat MC, Alvarenga TM, Silva MS, Alarie Y (2016) First larval description and chaetotaxic analysis of the neotropical whirligig beetle genus *Enhydrus* Laporte (Coleoptera, Gyrinidae). Revista Brasileira de Entomologia 60(3): 231–237. https://doi.org/10.1016/j.rbe.2016.05.005

Otis GW, Taylor BA, Mattila HR (2023) Invasion potential of hornets (Hymenoptera: Vespidae: *Vespa* spp.). Frontiers in Insect Science 3: 1145158. https://doi.org/10.3389/finsc.2023.1145158

Perrard A, Lopez-Osorio F, Carpenter JM (2016) Phylogeny, landmark analysis and the use of wing venation to study the evolution of social wasps (Hymenoptera: Vespidae: Vespinae). Cladistics 32(4): 406–425. https://doi.org/10.1111/cla.12138

Reid JA (1942) On the classification of the larvae of the Vespidae (Hymenoptera). Transactions of the Entomological Society of London 92(2): 285–331. https://doi.org/10.1111/j.1365-2311.1942.tb01208.x

Requier F, Fournier A, Pointeau S, Rome Q, Courchamp F (2023) Economic costs of the invasive Yellow-legged hornet on honey bees. Science of the Total Environment 898: 165576. https://doi.org/10.1016/j.scitotenv.2023.165576

Royle NJ, Smiseth PT, Kölliker M [Eds] (2012) The evolution of parental care (1st ed.). Oxford University Press. https://doi.org/10.1093/acprof:oso/9780199692576.003.0001

Schmidt JO (2018) Clinical consequences of toxic envenomations by Hymenoptera. Toxicon 150: 96–104. https://doi.org/10.1016/j.toxicon.2018.05.013

Schultner E, Oettler J, Helanterä H (2017) The role of brood in eusocial Hymenoptera. Quarterly Review of Biology 92(1): 39–78. https://doi.org/10.1086/690840

Skvarla MJ, Bertone MA, Liesch PJ (2022) Murder hornet mayhem: the impact of the 2020 giant hornet panic and COVID-19 pandemic on arthropod identification laboratories. American Entomologist 68(2): 38–43. https://doi.org/10.1093/ae/tmac029

Smith-Pardo AH, Carpenter JM, Kimsey L (2020) The diversity of hornets in the genus *Vespa* (Hymenoptera: Vespidae; Vespinae), their importance and interceptions in the United States. Insect Systematics and Diversity 4(3): 2, 1–27. https://doi.org/10.1093/isd/ixaa008

Solodovnikov AY (2007) Larval chaetotaxy of Coleoptera (Insecta) as a tool for evolutionary research and systematics: less confusion, more clarity. Journal of Zoological Systematics and Evolutionary Research 45(2): 120–127. https://doi.org/10.1111/j.1439-0469.2006.00387.x

Spradbery JP (1973) Wasps: An account of the biology and natural history of social and solitary wasps. Seattle: University of Washington Press.

Tan JL, Duan MJ, Yin LF, Hao HW, Chen XX (2013) The pre-overwintering nests and the immature stages of the hornet *Vespa fumida* van der Vecht (Hymenoptera: Vespidae). Journal of Natural History 47(19–20): 1325–1337. https://doi.org/10.1080/00222933.2012.759286

Tsai CL, Fang CC, Chen WJ, Dierberg K (2005) Hornet sting-induced toxic hepatitis. Clinical Toxicology 43(2): 127–128. https://doi.org/10.1081/CLT-50386

van der Vecht J (1957) The Vespinae of the Indo-Malayan and Papuan areas (Hymenoptera, Vespidae). Zoologische Verhandelingen 34(1): 1–82.

Wenzel JW (2020) Nest structure: social wasps. Encyclopedia of Social Insects. Springer, Cham: 632–645. https://doi.org/10.1007/978-3-319-90306-4_146-1

Wheeler GC, Wheeler J (1976) Ant larvae: review and synthesis. Washington, D. C.: The Entomological Society of Washington.

Wilson TM, Takahashi J, Spichiger SE, Kim I, Van Westendorp P (2020) First reports of *Vespa mandarinia* (Hymenoptera: Vespidae) in North America represent two separate maternal lineages in Washington state, United States, and British Columbia, Canada. Annals of the Entomological Society of America 113(6): 468–472. https://doi.org/10.1093/aesa/saaa024

Yamane Sk (1976) Morphological and taxonomic studies on vespine larvae, with reference to the phylogeny of the subfamily Vespinae (Hymenoptera: Vespidae). Insecta Matsumurana New Series 8: 1–45. http://hdl.handle.net/2115/9782

Yamane Sk, Okazawa T (1981) Mature larvae of some polistine wasps from Papua New Guinea and Fiji, with notes on larval characters of the old world and oceanian Polistinae (Hymenoptera: Vespidae). Reports of the Faculty of Science, Kagoshima University (Earth Science, Biology) 14: 65–75. http://hdl.handle.net/10232/5930